Webpage Abstract

Earthquakes impact the safety and reliability of gas storage and transmission systems. Current risk studies performed by utility owners and operators are derived from risk scoring that is highly subjective and qualitative, which do not provide the framework for proper incorporation of uncertainties. The reliability of the risk assessments needs improvement through reducing uncertainties with quantitative data. A new open-source seismic risk assessment tool, *OpenSRA*, was developed to enable system regulators and operators to address challenges posed by the risk from earthquakes and to prioritize reliably the most impactful seismic retrofits for gas infrastructure in California. *OpenSRA* incorporates new methods to assess the seismic risk of gas infrastructure due to multiple geohazards, and it incorporates new seismic capacity ("fragility") curves for gas system components based on highly efficient modeling and laboratory testing supplemented by validation processes for more reliable assessments. *OpenSRA* provides an analysis framework grounded on a methodical performance-based quantitative approach instead of an ad hoc qualitative approach. With *OpenSRA*, assessments are built from robust quantitative data for seismic demand and seismic capacities of gas storage, pipeline systems, and its components.

CALIFORNIA ENERGY COMMISSION

CALIFORNIA NATURAL RESOURCES AGENCY

FINAL PROJECT REPORT

Performance-Based Earthquake Engineering Assessment Tool for Natural Gas Storage and Pipeline Systems

Agreement Number: PIR-18-003

Author(s):
Jonathan Bray and Norman Abrahamson
University of California at Berkeley

Jennie Watson-Lamprey and Micaela Largent
Slate Geotechnical Consultants, Inc.

California Energy Commission Project Manager:
Yahui Yang
Energy Research and Development Division

Table of Contents

Executive Summary

This report summarizes the activities and accomplishments of the Performance-Based Earthquake Engineering (PBEE) Assessment Tool for Gas Storage and Pipeline Systems project. It describes the project components, the framework of the Open-source Seismic Risk Assessment (*OpenSRA)* software, and the resulting seismic capacity ("fragility") curves. Three gas systems are considered in this study: a) buried pipelines, b) underground storage facilities, and c) aboveground storage and transmission systems. The hazards of surface fault rupture, earthquake ground shaking, liquefaction-induced ground movements, and earthquake-induced landslides are also characterized in this study. The seismic hazard assessments and the finite element modeling results are used to develop fragility curves that are implemented into *OpenSRA* to aid end users in evaluating the seismic performance of their systems to prioritize risk mitigation efforts.

Background

Earthquakes directly impact the safety and reliability of gas storage and transmission systems. Current risk studies performed by gas utilities are derived from risk scoring that is highly subjective and qualitative. One of the main concerns of current risk assessment practices is the uncertainty introduced by subjectivity, lack of data, and poorly defined demand models. To improve the reliability of the risk assessments, uncertainties need to be reduced with quantitative data. This project reduces and defines the uncertainties associated with typical risk assessment by defining demand models for different levels of data (e.g., more data reduces uncertainty). This project's research also expands the knowledge of the seismic capacity, or fragility, of gas infrastructure.

A methodical and rational approach to implementing mitigation increases safety. System-wide fragilities and prioritization of mitigation will provide greater reliability of the overall system. Mitigation decisions based on robust quantitative data can be directed to focus efforts, resulting in effective disbursement and lower overall costs. Vulnerable system components can be repaired or strengthened before failure, avoiding adverse environmental impacts, and supporting public health and energy security.

Project Purpose and Approach

The overall goal of the *OpenSRA* Project is to create an open-source research-based seismic risk assessment tool for gas infrastructure that can be used by utility stakeholders to better understand state-wide risks, prioritize mitigation, plan new gas infrastructure, and help focus post-earthquake repair work. *OpenSRA*, has been developed to enable system regulators and operators to strategically address challenges posed by the risk from earthquakes and to prioritize reliably the most impactful seismic retrofits for the gas infrastructure in California.

The project team includes researchers from University of California (UC) Berkeley, LBNL, UC San Diego, University of Nevada Reno, the Natural Hazards Engineering Research Infrastructure (NHERI) SimCenter at UC Berkeley, and Slate Geotechnical Consultants (Slate) and its subcontractors Lettis Consultants International (LCI) and Professor Thomas O'Rourke of Cornell University.

Within the development process, different research task groups estimated the different probabilities required within the PBEE framework of Moehle and Deierlein (2004). The seismic

demands that were assessed were ground shaking, fault displacement, liquefaction-induced lateral spreading, liquefaction-induced settlement, and seismic-induced landsliding. The components of the gas infrastructure that were considered were wells and caprocks, aboveground infrastructure, and buried pipelines. The seismic demands (such as ground shaking or displacement due to an earthquake) and seismic capacities (fragilities) were then implemented into the open-source software *OpenSRA* to help regulators and utility owners calculate the probability of failure occurring in their system.

To monitor successful progress of this project, the following metric goals were established at the beginning of the project: website clicks, User Workshop attendance, lab testing goals, and validation results.

Key Results

The primary result of this project is the *OpenSRA* software. It is available to the public through the PEER website. The *OpenSRA* software addresses several of the concerns associated with the ad hoc manner in which current seismic risk assessments of gas pipelines and storage facilities are performed.

Improved models of earthquake-induced ground failure hazards (i.e., liquefaction-induced lateral spreading and earthquake shaking-induced landslides) were developed to better capture these hazards at different levels of regional scale analysis. The uncertainty assigned to the ground failure hazard models at different regional scales is consistent with the information available in California at the state-wide, regional, and site-specific levels.

Experiments of pipe components and subsystems provided critical insights on their seismic performance. Advanced analysis of gas storage wells identified key response characteristics and insights on their seismic performance. New sensing technologies were identified and reviewed which can inform the risk models at the input, intermediate, and final output stages. Validation of the models and software was conducted at four demonstration sites, and analysis results correlated well with documented observations after specific earthquakes (Bain et al., 2023).

Knowledge Transfer and Next Steps

The dissemination of information during the project has been implemented with the goal of informing users of the project methodology and results. The outreach effort ensures that knowledge transfer is coordinated to optimize dissemination of the research results and that *OpenSRA* has the best chance of being adopted in industry. Knowledge transfer was initiated with the development of a project logo, project website (https://peer.berkeley.edu/opensra) that is the public's main point of entry to the project, and a central repository that is continuously updated with the research goals, tasks, findings, and development of *OpenSRA*. More information on knowledge transfer can be found in Kang et al. (2023). Notifications of research findings and their significance to the *OpenSRA* software were issued by PEER electronic newsletters and social media channels (LinkedIn, Twitter, and Facebook).

Presentations about the project, research basis, and applications were made at workshops and conferences targeted to other natural hazards engineering researchers, practitioners, and stakeholders/users. Most notably, the project's progress was featured in a special technical session,"Seismic Risk Assessment Methodologies and Open-Source Tools for Natural Gas Infrastructure," at the 12th National Conference on Earthquake Engineering (12NCEE). These

presentations are summarized on the project website at https://peer.berkeley.edu/opensra/related-news.

During the project's development, meetings were held with a Technical Advisory Committee (TAC) which is composed of representatives from CEC, California Geologic Energy Management Division (CalGEM), California Public Utilities Commission (CPUC), and user utilities such as SoCalGas and PG&E. The TAC helped set the project team's research objectives, provided insights into industry technical needs, and asked probing questions during five TAC meetings. A User Workshop was also held to facilitate the use and broader application of the software tool. The User Workshop had around 80 registrations globally, with 31 in-person attendees.

Finally, the project team has been meeting with PG&E and SoCalGas, providing the software tool demonstrations, and discussing their needs throughout the project. This will enable further conversations to continue and potential adoption of the *OpenSRA* software.

Future development of *OpenSRA* would benefit from additional research in the following general areas:

- Pipeline response to additional geometric configurations, or to support variations such as pipelines attached to bridges
- Extend numerical models of soil-pipeline response for additional loading scenarios
- Optimize updating of models using information from sensing technologies installed on infrastructure systems
- Integration with USGS ShakeMap scenarios, more complex rupture scenarios, or other forms of natural hazards
- Integration into infrastructure types that have upstream/downstream interdependencies
- Development of the software backend for computational efficiency as enhancements are added to the software.
- Extension of the software to web-based use for broader access.

The expanded use of *OpenSRA* will continue to be informed by input and feedback from user-driven needs and applications that provide data needed for decision making.

Introduction

The current state of practice for seismic risk assessment of gas infrastructure includes risk scoring approaches, which are highly subjective and qualitative. These methods either do not estimate/incorporate uncertainties; require the user to estimate them based on outdated data and engineering judgement; or greatly overestimate uncertainties due to lack of data. This can lead to an incorrect estimation of seismic risk and probability of failure for the system. Additionally, current tools lack transparency, i.e., utility stakeholders often do not know how the risk assessment is being performed. These concerns are addressed through the updated methodologies, incorporation of uncertainties, and open-source nature of this project and the software created.

The overall goal of the *OpenSRA* Project is to create an open-source research-based seismic risk assessment tool for gas infrastructure that can be used by utility stakeholders to better understand state-wide risks, prioritize mitigation, plan new gas infrastructure, and help focus post-earthquake repair work. This is achieved by conducting user-driven research to develop a comprehensive quantitative seismic risk methodology using probabilistic data to evaluate and manage the seismic risk for gas storage and pipeline systems. To monitor successful progress of this project, the following metric goals were established at the beginning of the project: website clicks, User Workshop attendance, lab testing goals, and validation results. These metrics are associated with project exposure, interest and utilization of the software, and improvement of calculation methods.

The probabilistic seismic risk tool developed in this project follows the widely accepted risk methodology of Cornell (1968). A seismic source characterization is used to develop a suite of earthquake scenarios with associated rates of occurrence to represent the seismic hazard. Fault ruptures and the resulting ground shaking are generated for each earthquake scenario to represent the seismic loading, which includes a map of ground motion parameters. This scenario-based seismic parameter map is overlaid on the infrastructure system, and the seismic loading is related to the capacities of the infrastructure to calculate the seismic performance of the gas system for the scenario. By repeating the process for all the scenarios in the suite, the tool can evaluate the seismic risk to the system.

OpenSRA was developed to be applied easily by regulators and utility owners, and to include updated models and methods for the seismic demands and capacities that control the seismic risk for gas systems; this was done by including the users (utility owners and operators) from the onset. The project includes several innovative approaches that improve the basic methodology and distinguish this project's approach from standard approaches currently used. Current risk studies developed by the utilities use risk scoring approaches that are highly subjective and qualitative. They do not properly incorporate the uncertainties in the seismic demand and in the fragility of the system and its components. Targeted research, including liquefaction, landsliding, fault displacement, and fragility of different components of infrastructure, was conducted in this project to improve the characterization of uncertainty of key inputs to the seismic risk assessment tool. The methodology employed in this project provides quantitative estimates of the probabilistic seismic risk.

This report summarizes the activities and accomplishments of the *OpenSRA* project. It provides a high-level outline of the project components, framework of the *OpenSRA* software, and the resulting fragility

curves. Three gas systems are considered in this study: a) buried pipelines, b) underground storage facilities, and c) aboveground storage and transmission systems. The hazards of surface fault rupture, earthquake ground shaking, liquefaction-induced ground movements, and earthquake-induced landslides are characterized in this study. Three levels of analysis may be performed depending on the quantity and quality of data available and the sophistication of the model that can be used for each data level. Each component of the system has undergone finite element modeling to estimate the response of the component to the ground shaking and ground deformation resulting from each hazard and resulting the probability of failure. The seismic hazard assessments and the finite element modeling results developed as part of this study are used to develop fragility curves that are implemented into *OpenSRA* to aid end users in estimating failures in their systems as well as prioritizing risk mitigation efforts.

Project Approach

Background

The culminating product of this multi-year project is the *OpenSRA* software. This software is comprised of seismic demand and seismic capacity ("fragility") analyses. Multiple research efforts were undertaken to address these two analysis types as well as studying the different subsystems and components of gas infrastructure. The *OpenSRA* framework serves as a roadmap for the different elements making up the software. This section will describe the framework of *OpenSRA*, the demand analyses performed to reach the final results, and the approach used to calculate fragilities and validate the program. It should be noted that this report provides an overview of a large and multi-disciplinary project. As such, many of the sections will provide references to the CEC reports completed earlier in the project. For more specific information about each of the following sections please refer to these previous reports.

Multiple organizations contributed to this project to perform all the necessary components. The project team includes researchers from University of California (UC), Berkeley; Lawrence Berkeley National Lab (LBNL); UC San Diego (UCSD); University of Nevada Reno (UNR), the Pacific Earthquake Engineer Research (PEER) Center, the National Hazards Engineering Research Infrastructure (NHERI) SimCenter, and Slate Geotechnical Consultants and its subcontractors Lettis Consultants International (LCI) and Thomas O'Rourke of Cornell University.

Focused research to advance the seismic risk assessment tool was conducted by task groups, each addressing a particular area of study and expertise, and collaborating with the other groups. The Tasks are as follows:

Task A: Fault displacement
Task B: Liquefaction-induced deformation and seismically induced slope displacement
Task C: Performance of gas storage well casings and caprock
Task D: Performance of gas storage and pipeline system surface infrastructure
Task E: Smart gas infrastructure sensing of wells and pipeline connections performance
Task F: Synthesis of component fragilities into a system performance model

Targeted research was conducted in this project to improve the characterization of the uncertainty of key inputs. The uncertainties are further defined with levels of analysis. Three levels of analysis may be performed depending on the quantity and quality of data available and the sophistication of the model that can be used for each data level. Level 1 is a statewide analysis, Level 2 is a regional analysis, and Level 3 is a site-specific analysis. Each component of the system has undergone finite element modeling to estimate the response of the component to the ground shaking and ground deformation resulting from each hazard and resulting the probability of failure.

OpenSRA

OpenSRA is an open-source seismic risk assessment tool developed to assess the seismic risk of gas infrastructure. As mentioned previously, the software implements the six task groups outlined above to calculate the seismic demand, damage, and risk of failure for gas

systems. The following sections outline the framework, calculation components, and highlights the new-to-industry calculation methods utilized within *OpenSRA*.

Framework

OpenSRA follows the Performance-Based Earthquake Engineering (PBEE) risk methodology developed by PEER (Moehle and Deierlein, 2004) to assess the seismic risk of gas infrastructure. The PBEE risk methodology uses a combination of probabilities to calculate the risk of a "decision variable" occurring. These calculations can be lengthy as there are multiple probability density functions to not only calculate but to integrate over to develop estimates and their uncertainty. To perform the calculations within *OpenSRA* in a timeframe that will be useful to the user, Polynomial Chaos (PC) has been implemented. This methodology requires clearly defined means, aleatory variabilities, and epistemic uncertainties for each step of the PBEE risk methodology. For more detailed information regarding *OpenSRA* and PC please refer to Zheng et al. (2023).

Efficient Evaluation of the PBEE Risk Framework

The risk framework is simply presented as a triple integral below (Equation 1) adapted from Moehle and Deierlein (2004).

$$\lambda_{dv} = \int_{DM} \int_{EDP} \int_{IM} P\{DV > dv|dm\}\, p\{dm|edp\}\, p\{edp|im\}\, \lambda_{im} d(im) d(edp) d(dm) \qquad (1)$$

In the above equation, IM is the intensity measure (e.g., peak ground acceleration), EDP is the engineering demand parameter (e.g., ground deformation), DM is the damage measure (e.g., pipe strain), DV is the decision variable (e.g., rate of rupture), λ is the annual rate, the operations of $p\{y|x\}$ and $P\{Y > y|x\}$ are the conditional probability density function (PDF) and cumulative distribution function (CDF), respectively, of y given x. Given these definitions, λ_{IM} is the annual rate of occurrence of the seismic event, $p\{edp|im\}$ is the probability of a system response computed using geohazard models given the seismic demand, $p\{dm|edp\}$ is the fragility assessment given the system response, and $p\{dv|dm\}$ is the loss estimate given the damage level.

The method presented by Lacour and Abrahamson (2021) approximates PDFs and CDFs as linear combinations of a set basis functions (analogous to Taylor expansion of analytical functions), which are then incorporated into the analytical solution mentioned previously. The primary computation required for PC is the intermediate calculation of the PC terms, which are functions of the various σ_Y and σ_{μ_Y} for IM, EDP, DM, DV, and the linear approximation coefficients for EDP, DM, DV. This set of intermediate calculations is very fast and efficient to perform, because the PC terms are evaluated analytically. Furthermore, the polynomial functions are known mathematical functions, and the sampling of the uncertainty is performed only once during post-processing after the PC terms have been fully computed for all events. Overall, as discussed in Lacour and Abrahamson (2021), the use of PC over traditional Monte-Carlo sampling can easily improve the computation time by two to three orders of magnitude. For additional details to the application of PC to the risk framework and validation examples, please refer to the Lacour and Abrahamson (2023).

OpenSRA Overview

Given the PBEE framework, each of the research tasks has split their approaches to fulfill each of the probabilities. **Error! Reference source not found.** to Figure 3 show the workflow of *OpenSRA* and how the PEER risk methodology shown in Equation (1) is conceptually incorporated into the seismic risk assessment of each of the three infrastructure types: below ground pipelines, wells and caprocks, and aboveground subsystem components (Task B, C, and D respectively). The PEER risk methodology serves as the backbone to the *OpenSRA* risk assessment workflow. The user defines the infrastructure type that will be analyzed by *OpenSRA* and inputs their component characteristics. *OpenSRA* then steps through the PEER risk methodology as shown in the flow charts in these figures to perform the risk assessment.

As shown in **Error! Reference source not found.**, the workflow for below ground pipelines capture the influence of seismic intensity on ground deformation, the influence of ground deformation on pipe strain, and finally the influence of pipe strain on the probability of failure in the form of failure and leakage. The models to relate seismic intensity to ground deformation are based on state-of-the-art models that have been published in literature (Bain et al. 2022). The models to relate deformation to pipe strain and pipe strain to failure are developed as part of the focus of Task B and Task F. These models are described in detail in the following sections.

Figure 1: PEER Risk Methodology Applied to Below-Ground Pipelines

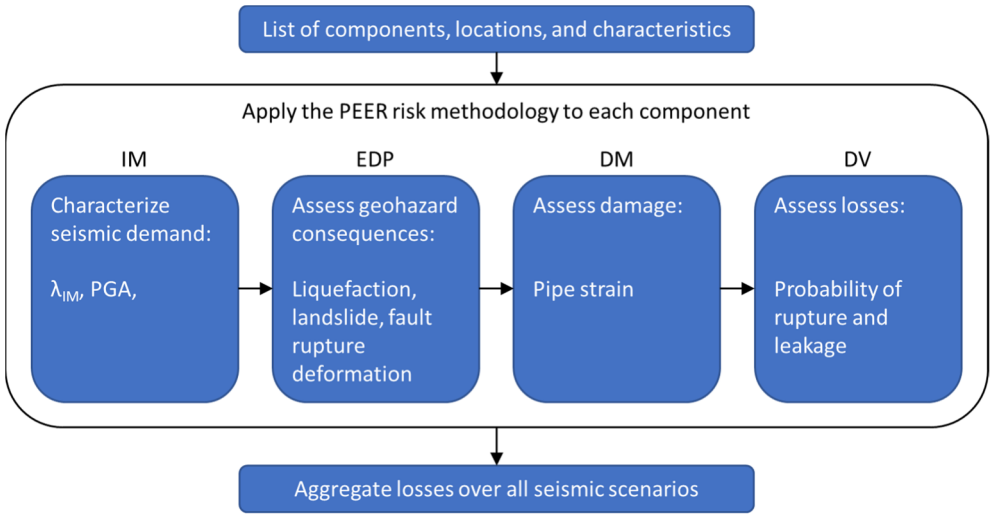

Source: Zheng et al. (2023)

Figure 2 shows the workflow for wells and caprocks. For this category, Task Groups C and F developed damage models for well casings and tubings that are dependent on fault rupture deformation and ground shaking. These models are considered as two independent modes of failure for wells. For caprocks, results of the numerical study suggest that probability of leakage is not significantly dependent on the tested model parameters, hence its distribution is independent on seismic and geohazard demands, and the overall risk is a constant distribution.

Figure 2: PEER Risk Methodology Applied to Wells and Caprock

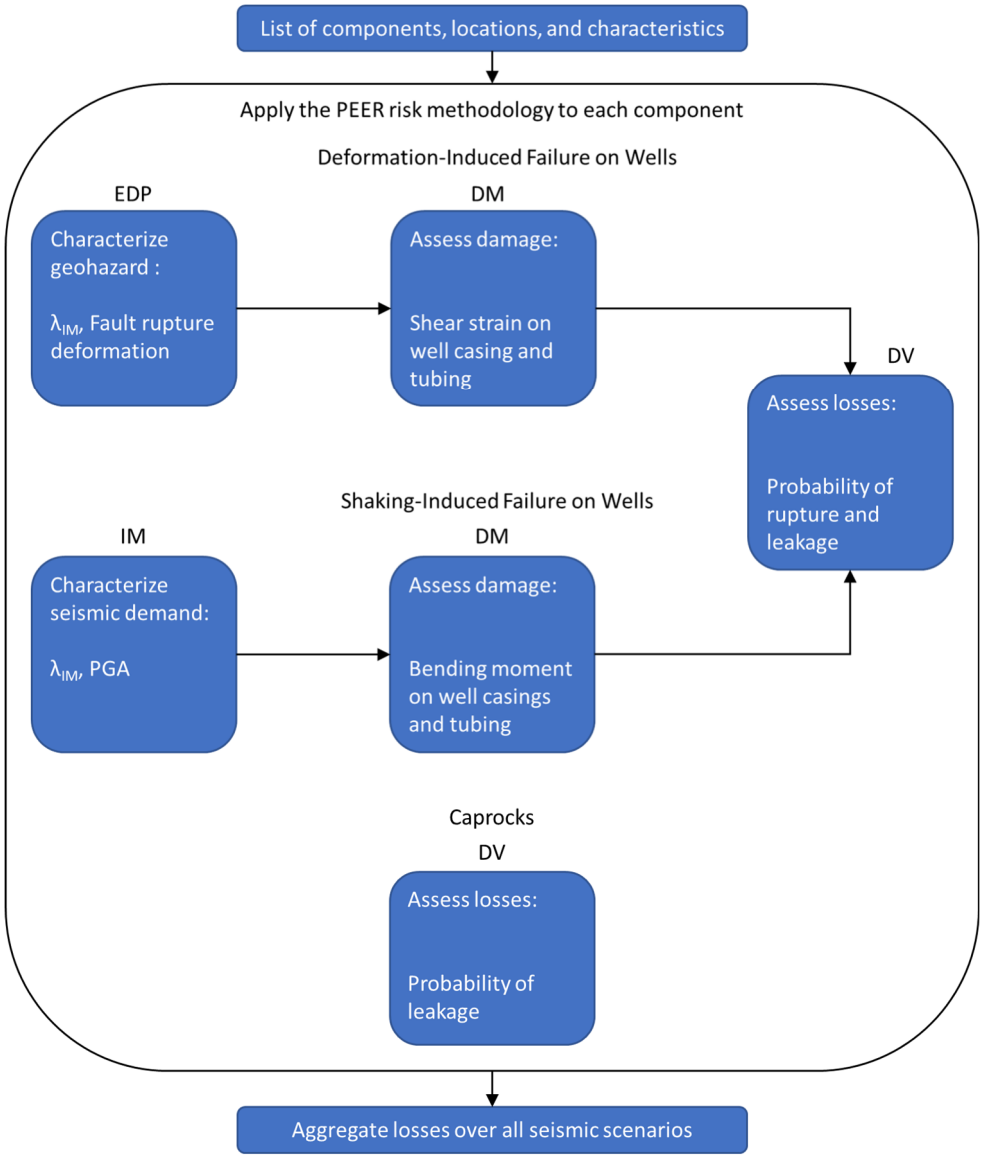

Source: Zheng et al. (2023)

Figure 3 shows the workflow for aboveground subsystem components, specifically failure associated with wellheads and pressure vessels. Research by Task D and F resulted in models for joint rotations and strains for wellheads and moment ratios for pressure vessels, both of which are dependent on the seismic intensity (i.e., peak ground acceleration). The intensity of the strains and moment ratios are then used to inform the levels of failure associated with wellheads and pressure vessels respectively.

Figure 3: PEER Risk Methodology Applied to Aboveground Components

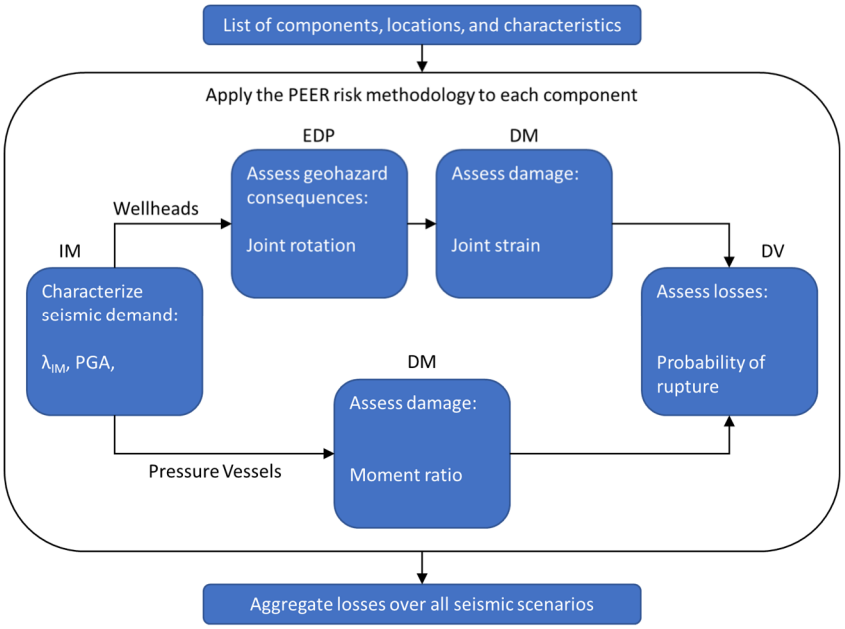

Source: Zheng et al. (2023)

Figure 4 shows a flow chart of the overall user process for *OpenSRA* and how the PEER risk framework is wrapped into the user experience. The user starts with entering general information, and selecting if the default values should be used for their analysis. Once these items, and more specific information (if not using the default values) is entered, the user can run the analysis and visualize the results.

Figure 4: OpenSRA User Experience Flow Chart

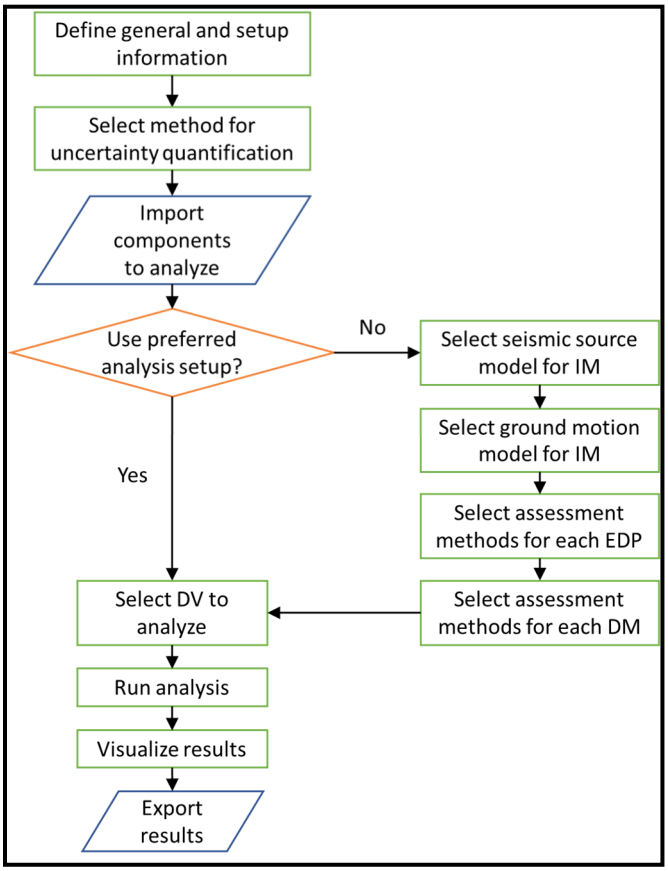

Source: Zheng et al. (2023)

Seismic Hazard Characterization

The ground shaking at a site is estimated by performing a probabilistic seismic hazard analysis (PSHA) using a combination of UCERF3.1 scenarios and ground motion models (GMMs) presented in the Next Generation Attenuation Relationships for Western US (NGA-West2) Project. The PSHA is performed in a preprocessing step that follows the approach first developed by Cornell (1968) with the inclusion of parameters for randomization and the consideration of epistemic uncertainty.

The seismic hazard (and therefore estimated ground motion) is calculated within *OpenSRA*. Similar to the fault displacement hazard (described in the next section), the rupture scenarios are determined using UCERF3.1. Running the entire list of rupture scenarios within *OpenSRA* would require a long computing time as it is comprised of 253,394 rupture scenarios. For the purposes of this hazard, the UCERF3.1 scenarios were reduced to 1194 scenarios with a magnitude step size 0.5. Additional information about the reduced list of rupture scenarios can be found in Lacour and Abrahamson (2023).

The ground motion is characterized by using a suite of four GMMs from NGA-West2. Ground motions can also be estimated directly by using ShakeMaps online (Wald et al. 2005). *OpenSRA* calculates the closest point of ground shaking (from ShakeMaps) to wherever the analysis bounds are located. Finally, users can also perform a deterministic scenario by defining a simple fault and using the same weighted NGA-West2 models.

Task 4a – Fault Displacement Hazard

A report titled "Fault Displacement Hazard Characterization for *OpenSRA*" by Thompson (2021) was previously submitted to CEC. Please refer to this report for additional details on the model. The primary goal of this subtask was to research models to estimate primary and secondary fault displacement hazard, and where this fault displacement hazard impacts underground pipelines, wells, and caprocks.

Throughout this report the seismic demands outlined are split up into levels. These levels correlate to the scale at which the analysis is performed and quantity of data available. Level 1 is a statewide analysis, Level 2 is a regional analysis, and Level 3 is a site-specific analysis. Guidance for implementing the fault displacement hazard element to *OpenSRA* for the various levels is captured in hazard matrix table in Thompson (2021). The recommended models, inputs, and outputs are presented in Table 1.

Table 1: Fault displacement models implemented into *OpenSRA*

Level	Model	Inputs	Outputs
Level 1	Wells and Coppersmith (1994)	UCERF3-linked Q-fault scenarios including: magnitude, dip, strike, rake	Fault displacement magnitude and direction
Level 2	Petersen et al. (2011)	UCERF3-linked Q-fault scenarios including: magnitude, dip, strike, rake	Fault displacement magnitude and direction
Level 3	PFDHA models (not yet public available)	Beyond the scope of this project	Fault displacement magnitude and direction

The fault-pipeline crossing algorithm for Levels 1 and 2 uses Q-faults (USGS and CGS, 2006) to map fault location while continuing to utilize UCERF3.1 for the rupture geometry (strike, dip, rake) and magnitude. A 100-meter buffer around the Q-fault traces defines the fault polygon and the nearest UCERF3 fault defines the rupture attributes. Figure 5 depicts the Q-fault locations along with pipeline crossings (shown with stars). Figure 6 shows both the primary and secondary fault zones developed by Thompson (2021). The pipeline shapefile is divided into straight, 100-meter segments to track the specific segments that cross fault zones. These mapped faults along with their calculated displacement vectors (described further in Zheng et al. (2023) are then utilized in the fragility development of buried pipelines, wells, and caprocks.

Figure 5: Intersections of Gas Pipelines in California with Fault Traces from the U.S. Quaternary Fault and Fold Database (2019 edition)

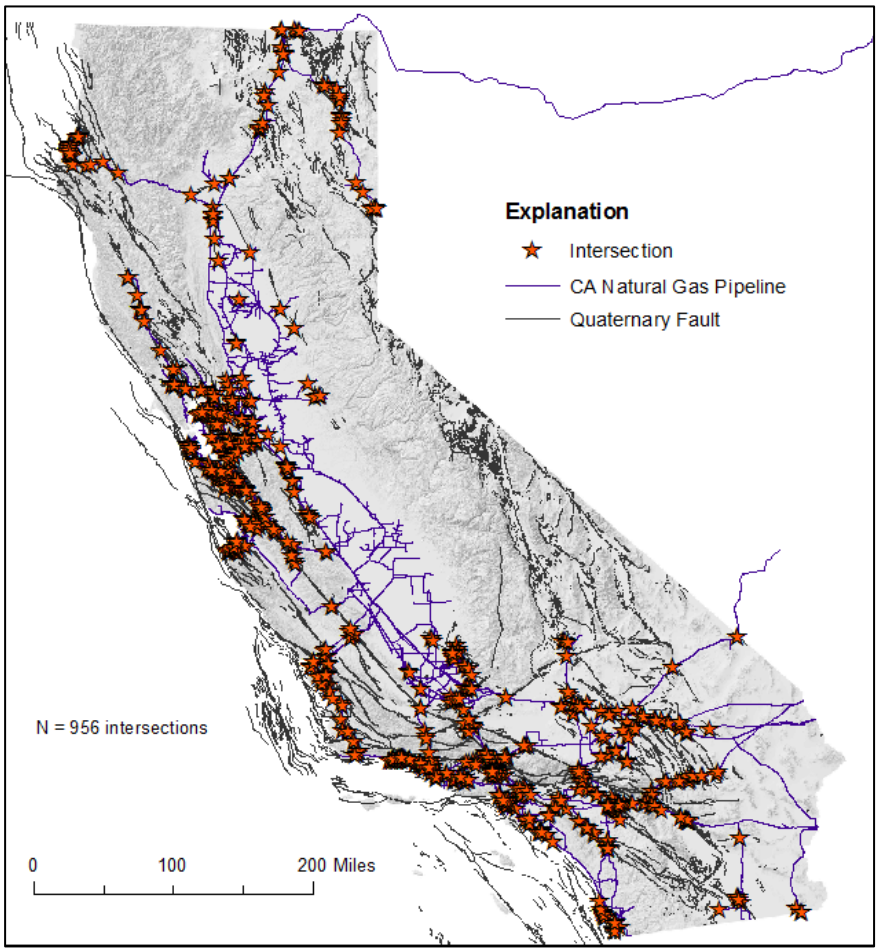

Map of California showing gas pipelines (in blue) and fault traces from the U.S. Quaternary Fault and Fold Database (in gray). The 956 intersections of these two linear datasets are indicated by red stars.

Source: Pipeline database from CEC. Fault source traces from USGS and CGS (2006).

Figure 6: Level 2 Primary and Secondary Fault Hazard Zones and California Pipelines in the San Francisco Bay Area

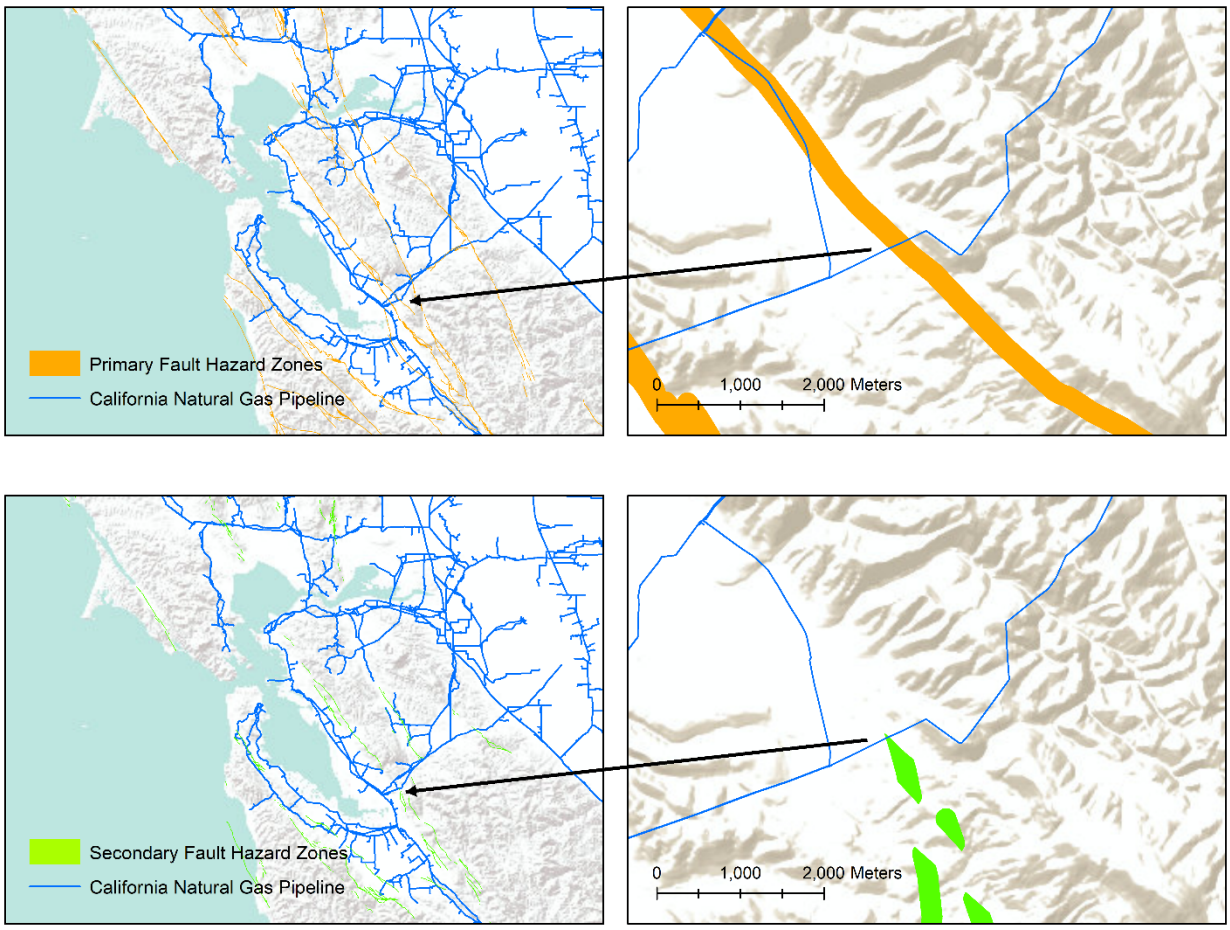

Primary (orange) and Secondary (green) fault hazard zones. Right side figures show examples of pipeline-fault zone intersections.

Source: Pipeline database from CEC. Fault source zones developed by Thompson (2021).

Task 4b – Liquefaction and Landsliding

A report titled "Enhanced Liquefaction and Ground Deformation Report" by Bain et al.(2022) was previously submitted to the CEC. Please refer to the previously submitted report for additional details on these models. This task group explored different earthquake-induced geohazards such as liquefaction, lateral spreading, and landsliding. Similar to Fault Displacement Hazard, these demands were split into different levels of analysis. Referring to Figure 1, this task group focused on estimating the EDP and DM for buried pipelines. The following sections outline the different EDP's considered (within this task group). The results of the damage model to predict strain (DM) will be presented in the "Results" section.

Liquefaction Triggering Models and Data

The models implemented into *OpenSRA* to calculate the probability of liquefaction are outlined in Table 2.

Table 2: Models for Liquefaction Triggering (Zheng et al. 2023)

Level	Model	Inputs	Model
Level 1	Zhu et al. 2017	PGV, V_{s30}, precipitation, D_c, D_r, D_w, GWT	Probability of liquefaction
Level 2	Youd and Perkins (1978) with Hazus (FEMA, 2020)	Surficial Quaternary geologic maps, PGA, M_w, GWT	Liquefaction susceptibility converted to probability of liquefaction
	Bain and Bray model (undergoing publication peer-review)	Surficial Quaternary geologic maps, PGA, M_w, GWT	Probabilistic assessment of liquefaction triggering and lateral spread displacement
Level 3	Boulanger and Idriss (2016)	CPT, PGA, M_w, GWT	Probability of liquefaction
	Probabilistic Modification to Robertson and Wride (1998) updated as Robertson (2009) from Ku et al. (2012)	CPT, PGA, M_w, GWT	Probability of liquefaction
	Moss et al. (2006)	CPT, PGA, M_w, GWT	Probability of liquefaction

Liquefaction-Induced Lateral Spread Displacement and Vertical Settlement Models and Data

Table 3 outlines the models for the probability of liquefaction-induced settlement. Table 4 outlines the models for lateral spreading. Specifically, for lateral spreading an updated Level 2 analysis is proposed to enable the use of enhanced data (when compared to Level 1). This method is briefly outlined below, and more information can be found in Bain et al. (2022).

At Level 2, the Hazus (FEMA, 2020) methodology can be applied to estimate potential lateral spread displacement and vertical settlement due to liquefaction. However, because enhanced data are available at Level 2 compared to Level 1, research has been performed to develop a new Level 2 procedure for assessing lateral spread displacement.

The proposed procedure is based on liquefaction probability curves for surficial geologic units, described in Holzer et al. (2011). This research has modified and expanded the framework of

the Holzer et al. (2011) procedure to include assessments for the probability of liquefaction triggering, potential lateral spread displacements, and estimates of their uncertainties. For further information on the development of this procedure please see Bain et al. (2022). An example of these expanded and updated curves are shown in

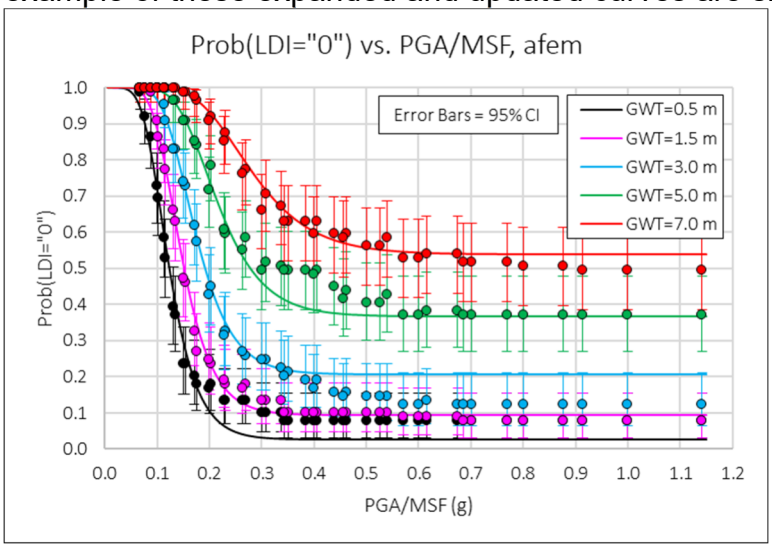

and Figure 8: Mean, Non-Zero LN(LDI) Data for afem Deposits

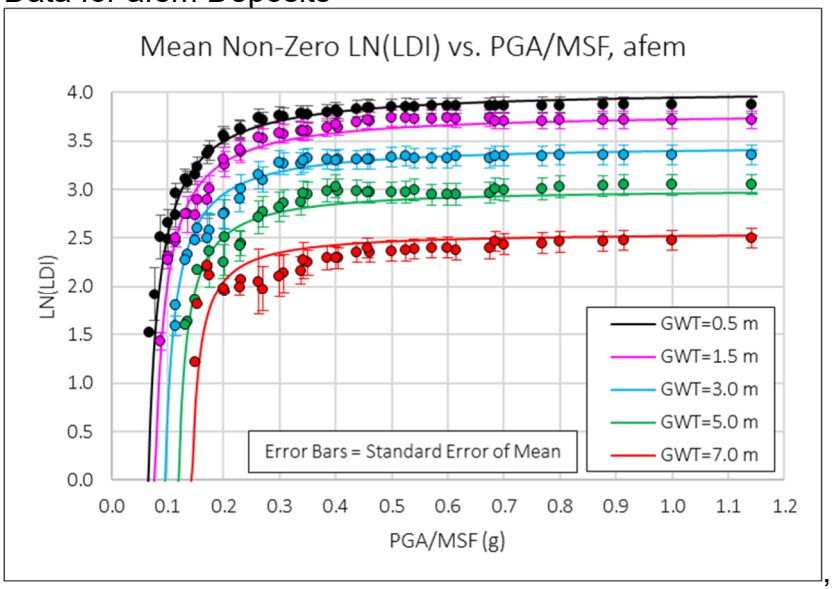

, where LDI is the lateral displacement index.

Table 3: Liquefaction induced settlement models implemented into *OpenSRA* (Zheng et al. 2023)

Level	Model	Inputs	Model
Level 1	Zhu et al. (2017) combined with Hazus (FEMA, 2020)	PGV, V_{s30}, precipitation, D_c, D_r, D_w, GWT	Liquefaction Susceptibility Class Converted to Settlement Estimate
Level 2	Zhu et al. (2017) with Hazus (FEMA, 2020)	PGV, V_{s30}, precipitation, D_c, D_r, D_w, GWT	Liquefaction Susceptibility Class Converted to Settlement Estimate
	Youd and Perkins (1978) with Hazus (FEMA, 2020)	Surficial Quaternary geologic maps, PGA, M_w, GWT	Liquefaction-induced settlement according to

			liquefaction susceptibility category
Level 3	Cetin et al. (2009)	SPT, GPA, Mw, GWT	Free-field, level-ground settlement
	Zhang et al. (2002)	CPT, PGA, Mw, GWT	Free-field, level-ground settlement

Table 4: Lateral spread models implemented into *OpenSRA* (Zheng et al. 2023)

Level	Model	Inputs	Outputs
Level 1	Zhu et al. (2017) with Hazus (FEMA, 2020)	PGV, V_{s30}, precipitation, D_c, D_r, D_w, GWT	Liquefaction susceptibility class converted to settlement estimate
Level 2	Youd and Perkins (1978) with Hazus (FEMA, 2020)	Surficial Quaternary geologic maps, PGA, M_w, GWT	Liquefaction susceptibility converted to lateral spread displacement
	Proposed model presented in Bain et al. (2022)	Surficial Quaternary geologic maps, PGA, M_w, GWT	Probabilistic assessment of liquefaction triggering and lateral spread displacement
Level 3	Zhang et al. (2004)	CPT, PGA, M_w, GWT, topographic slope or free-face ratio	Estimate of lateral spread displacement
	Idriss and Boulanger (2008) combined with Zhang et al. (2004)	CPT or SPT	Estimate of lateral spreading displacement

Figure 7: Prob(LDI="0") vs. PGA/MSF Data for afem Deposits

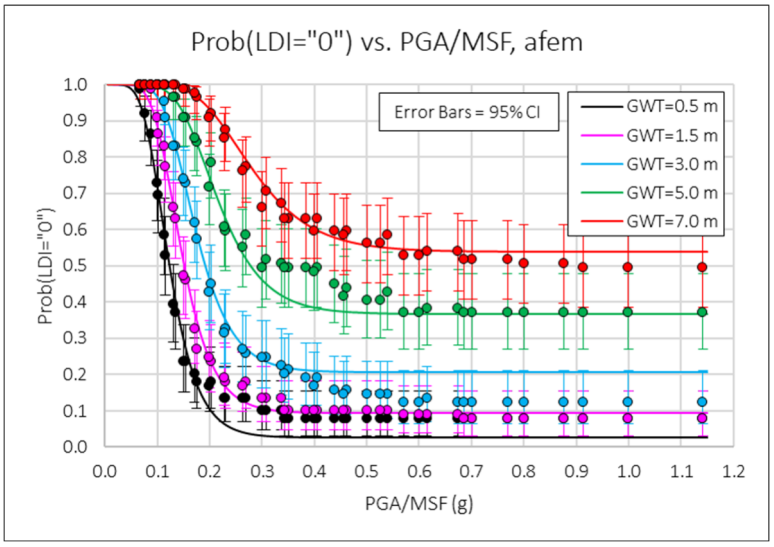

Fit of Prob(LDI="0") regression model to data calculated for sandy artificial fill over Bay Mud deposits
Source: Bain et al. (2022)

Figure 8: Mean, Non-Zero LN(LDI) Data for afem Deposits

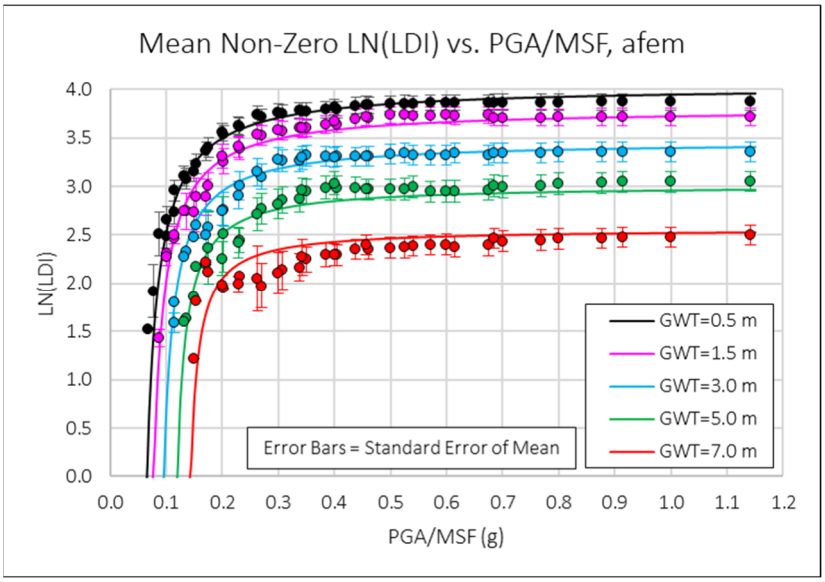

Fit of Mean, Non-Zero LN(LDI) regression model to data calculated for sandy artificial fill over Bay Mud deposits
Source: Bain et al. (2022)

The Prob(LDI=”0”) and non-zero LN(LDI) data (examples shown in

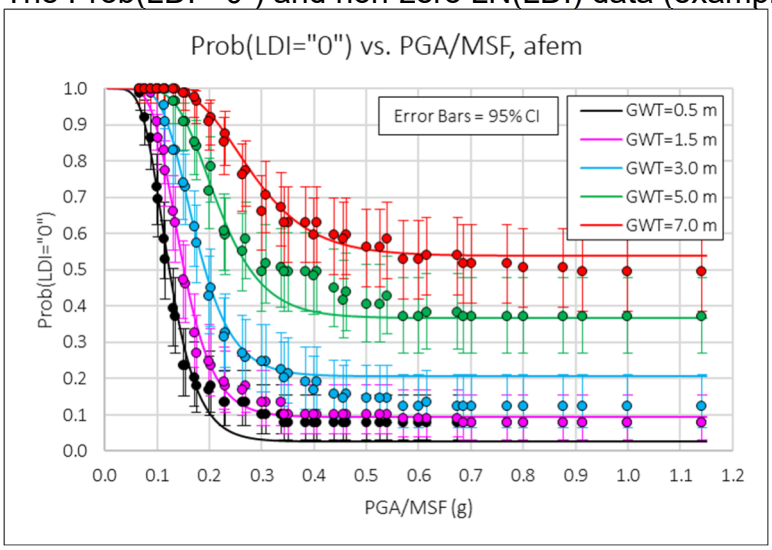

and Figure 8: Mean, Non-Zero LN(LDI) Data for afem Deposits

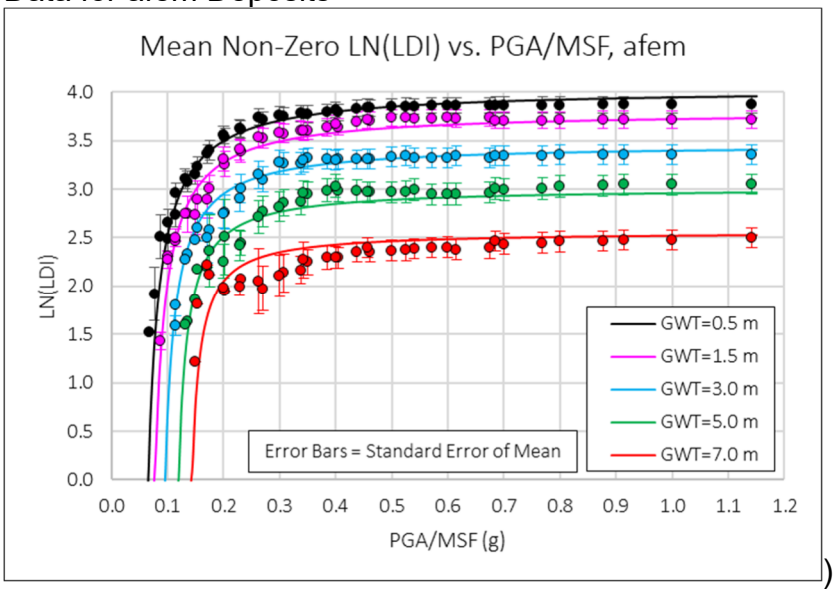

) are combined using a mixed-random variable model, as illustrated in

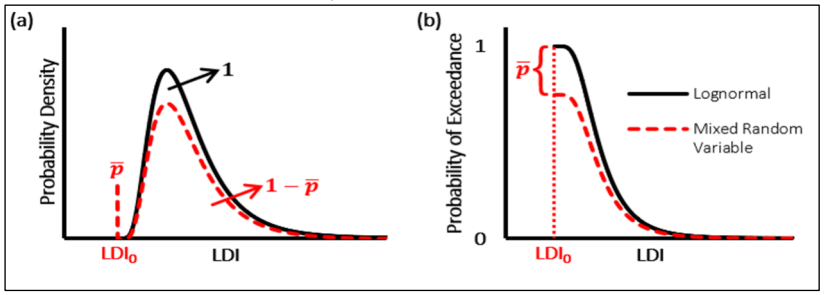

. These models estimate only a distribution of LDI. The estimated LDI distribution is converted to a distribution of lateral spread displacement using topographic correlations of LDI to lateral spread displacement (i.e., Zhang et al., 2004). Although this method has been shown to provide reasonable results in the San Francisco Bay Area and in Christchurch, New Zealand, it requires sufficient CPT data over an area to implement it in *OpenSRA*. At present this new procedure is only implemented in *OpenSRA* in the San Francisco Bay area.

Figure 9: Comparison of Continuous and Mixed Random Distributions

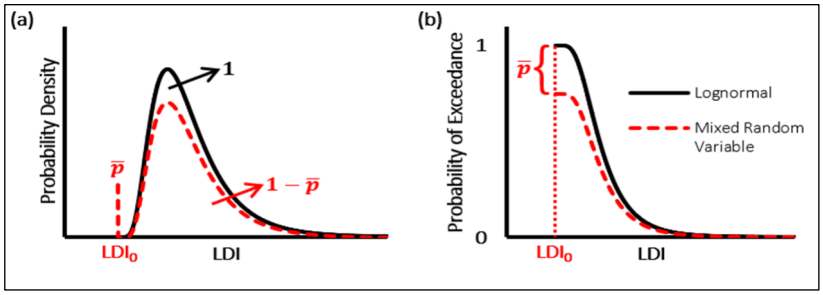

(a) PDF for a Mixed and Continuous Random Variable and (b) Probability of Exceedance for a Mixed and Continuous Random Variable
Source**:** Bain et al. (2022)

Seismic Slope Stability and Slope Displacement Models and Data

Table 5 outlines the proposed seismic-induced landsliding models that have been implemented into *OpenSRA*.

Table 5: Seismic-induced Landslide models implemented into *OpenSRA* (Zheng et al. 2023)

Level	Model	Inputs	Outputs
Level 1	Infinite slope analysis using strength distributions presented in Table B.15 in Bain et al. (2022)	Statewide Geologic Map	Estimate of Seismic Slope Displacement
Level 2	Grant et al. (2016)	topographic slope, ϕ, γ, c, c_r, t, PGA	Model predicts the type of slope movement (rock-slope failures, disrupted soil slides, coherent rotational slides, and lateral spreads) and estimates seismic slope displacement distribution
	Bray & Macedo (2019)	topographic slope, ϕ, γ, c, t, PGA, M_w	Seismic Slope Displacement Distribution
Level 3	Zhang et al. (2004)	CPT, PGA, M_w, GWT, topographic slope or free-face ratio	Estimate of lateral spread displacement
	Idriss and Boulanger (2008) combined with Zhang et al. (2004)	CPT or SPT	Estimate of lateral spreading displacement

Fragility Curve Development

Each research task was responsible for developing fragility curves for a specific component of gas infrastructure. This is represented in the PBEE framework in the “DM” and “DV” probabilities. More information can be found in (Watson-Lamprey et al., 2022).
Each research task performed sensitivity studies to find the input parameters that changed the probability of failure the most. Then defined the necessary inputs for their model, assigned ranges based on manufacturer guidance or expert opinion (mean and standard deviation), and

finally, changed each input individually (within its range) to see which parameters impacted the final answer. From there, the teams estimate damage models (i.e., probability of a strain level given an intensity measure) and fragility models (i.e., probability of failure given a strain or deformation), using a variety of laboratory testing and finite element modeling. These fragility curves are implemented into *OpenSRA* within each component calculation (underground pipelines, wells and caprocks, and surficial infrastructure). Further information on individual fragility curves is presented in the “Results” section of this report.

OpenSRA Validation and Use

Validation of *OpenSRA* is one of the key milestones of this project, and a crucial step in the technology transfer. Four sites were chosen to encapsulate the different geohazards, type of gas infrastructure at the site, and utility owners’ ability to give information to the team. These sites included Balboa Boulevard (a gas pipeline rupture occurred in the 1994 Northridge earthquake but there was no damage in the 1971 San Fernando earthquake), Cordelia Junction (which has a known landslide, based on confidential information shared by PG&E), McDonald Island (which has complex aboveground infrastructure, based on confidential information shared by PG&E), and Honor Rancho (which is close to many faults and has a large well field and caprock).

Each research team implemented their seismic demand and fragility models into *OpenSRA* and then performed analyses for past earthquakes or test earthquake scenarios to validate the program. More information on this can be found in (Bain et al. 2023).

Results

Introduction

This section outlines the results from the fragility curve development for the different subsystems (see the previously submitted interim project reports for further information regarding specific models and results). This section also includes information on the *OpenSRA* graphical user interface, where both the demand and fragility research is synthesized. Finally, project metrics are summarized.

Below Ground Pipelines

Referring to the *OpenSRA* framework and Figure 1, the previous section outlined the methods to estimate the EDP, and now given that EDP, this section focuses on how to estimate the DM. To do this, a numerical model of the soil-pipeline interaction and pipe response to permanent ground deformation was made using Abaqus Version 6.1. Details of the selected scenarios and numerical modeling techniques (e.g., finite element mesh, beam element type, springs, boundary conditions, integration points) are provided in the Hutabarat et al. (2023) report.

The numerical modeling in this study analyzed only abrupt ground movements (“knife-edge”). These result in locally higher strain concentrations compared to distributed ground movements, which were not studied.

Figure 10: Assessed Ground Deformation Modes

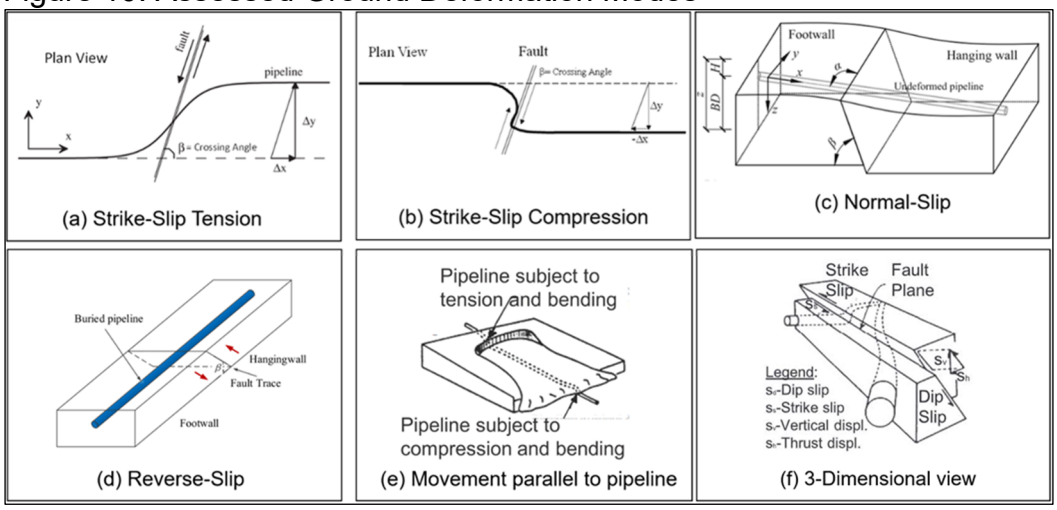

summarizes the ground deformation modes assessed for the *OpenSRA* Project. The following deformations were assessed:

- Pipelines that cross landslides or lateral spreads parallel to the direction of displacement
    - normal-slip (

- Figure 10: Assessed Ground Deformation Modes

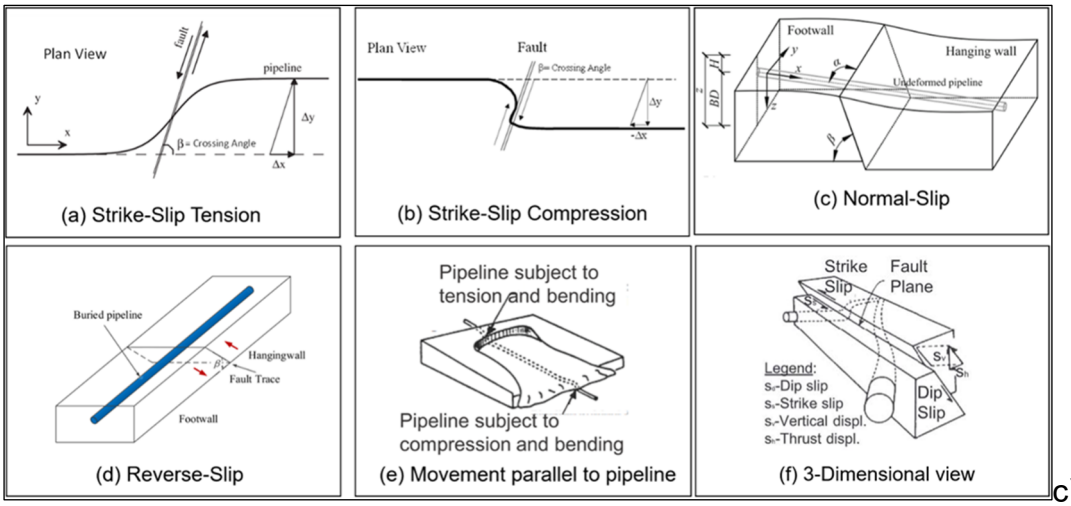

- c) at the scarp
- reverse-slip (

- Figure 10: Assessed Ground Deformation Modes
- 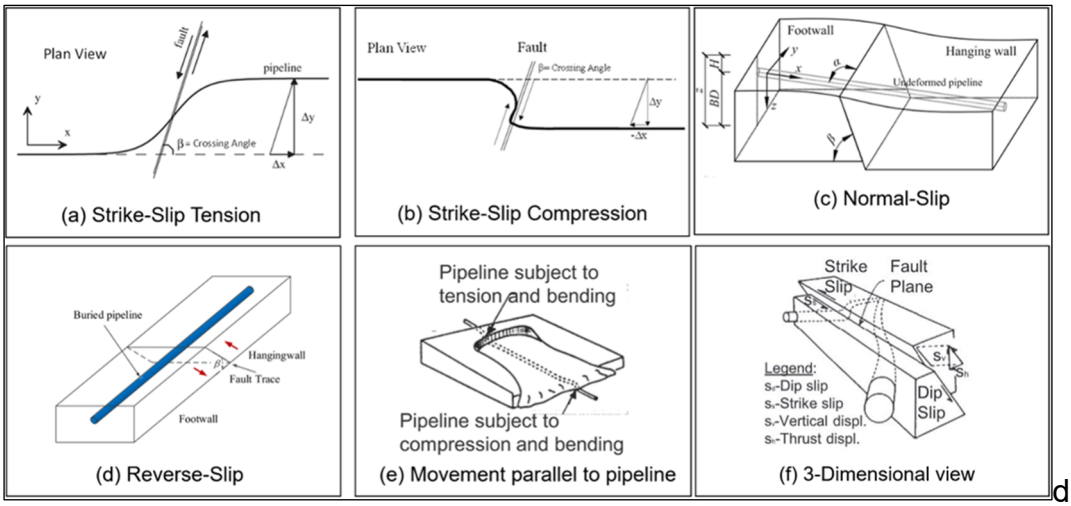

- d) at the toe
- the fifth case of ground deformation where no bending strains are induced (similar to

- Figure 10: Assessed Ground Deformation Modes
- 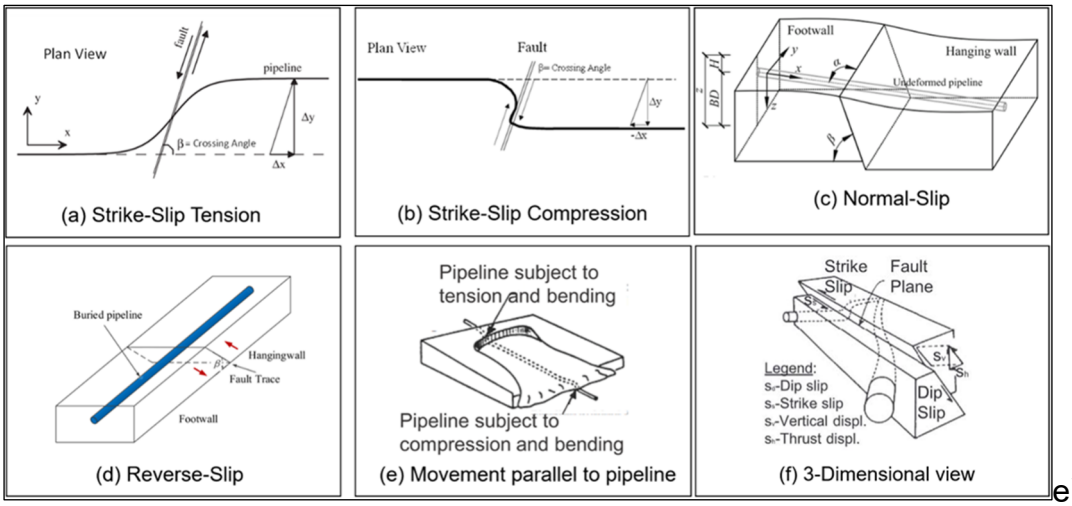

e)
- Pipelines that cross landslides or lateral spreads perpendicular or at an oblique angle
  - strike-slip tension (

- Figure 10: Assessed Ground Deformation Modes
- 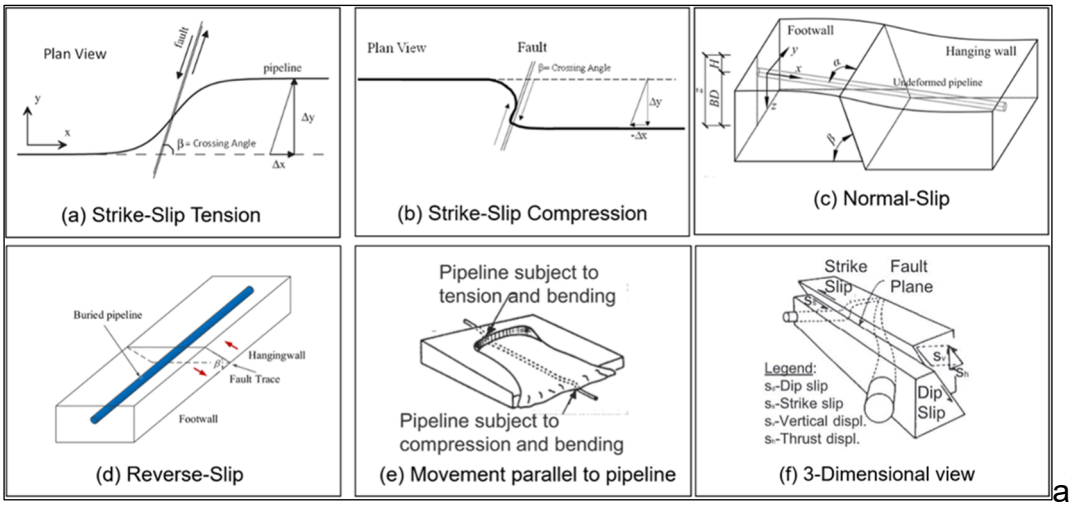

- a)
- strike-slip compression (

- Figure 10: Assessed Ground Deformation Modes
- 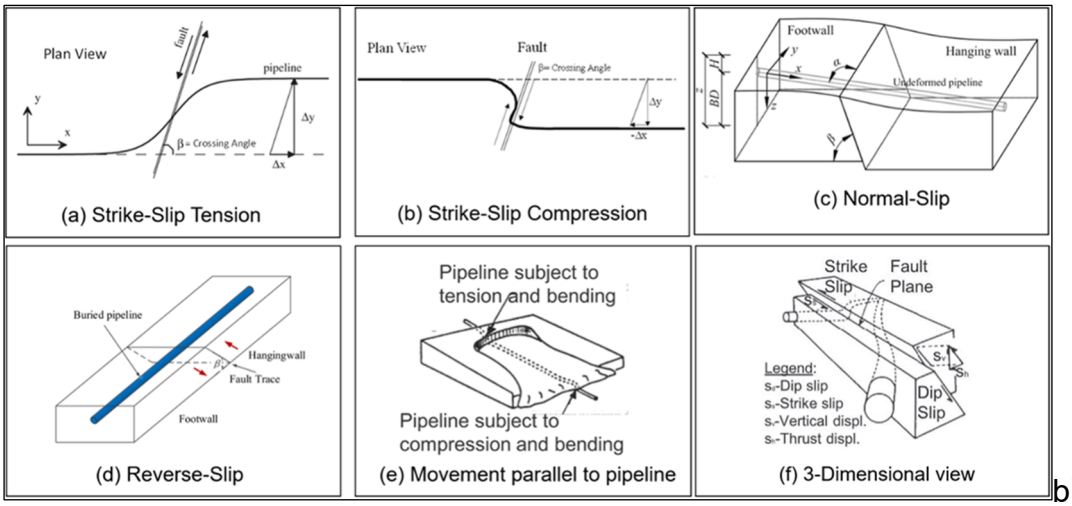

b)
- Ground settlement can be modeled as vertical normal-slip deformation (Figure 10c).

The complete results of the buried gas pipeline system modeling are provided in Hutabarat et al. (2023). Select plots of longitudinal pipe strain versus permanent ground deformation are displayed in
Source: Bain et al. (2022)

Figure 11.

Figure 10: Assessed Ground Deformation Modes

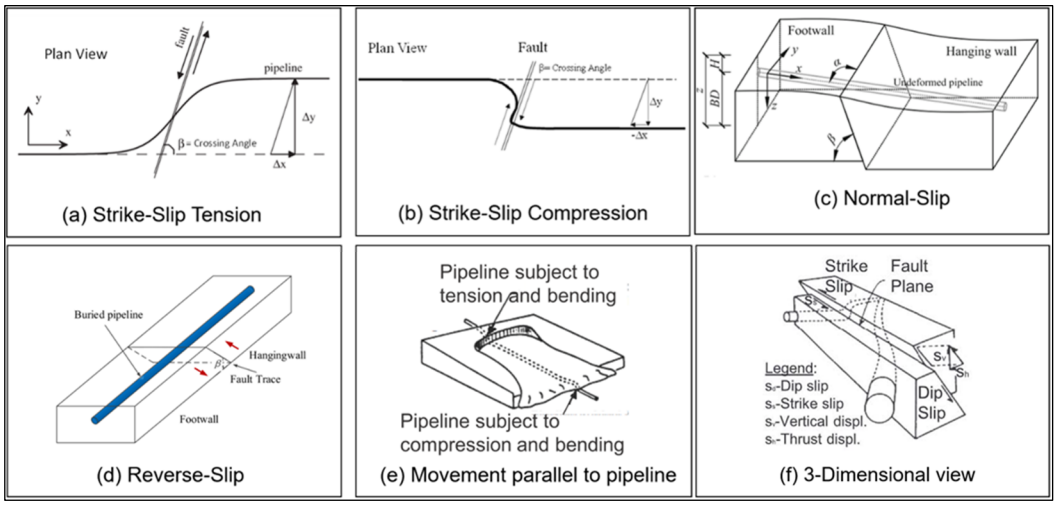

Ground deformation modes assessed to derive pipe strain fragility models
Source: Bain et al. (2022)

Figure 11: Longitudinal Pipe Strain versus Ground Deformation Simulation Results

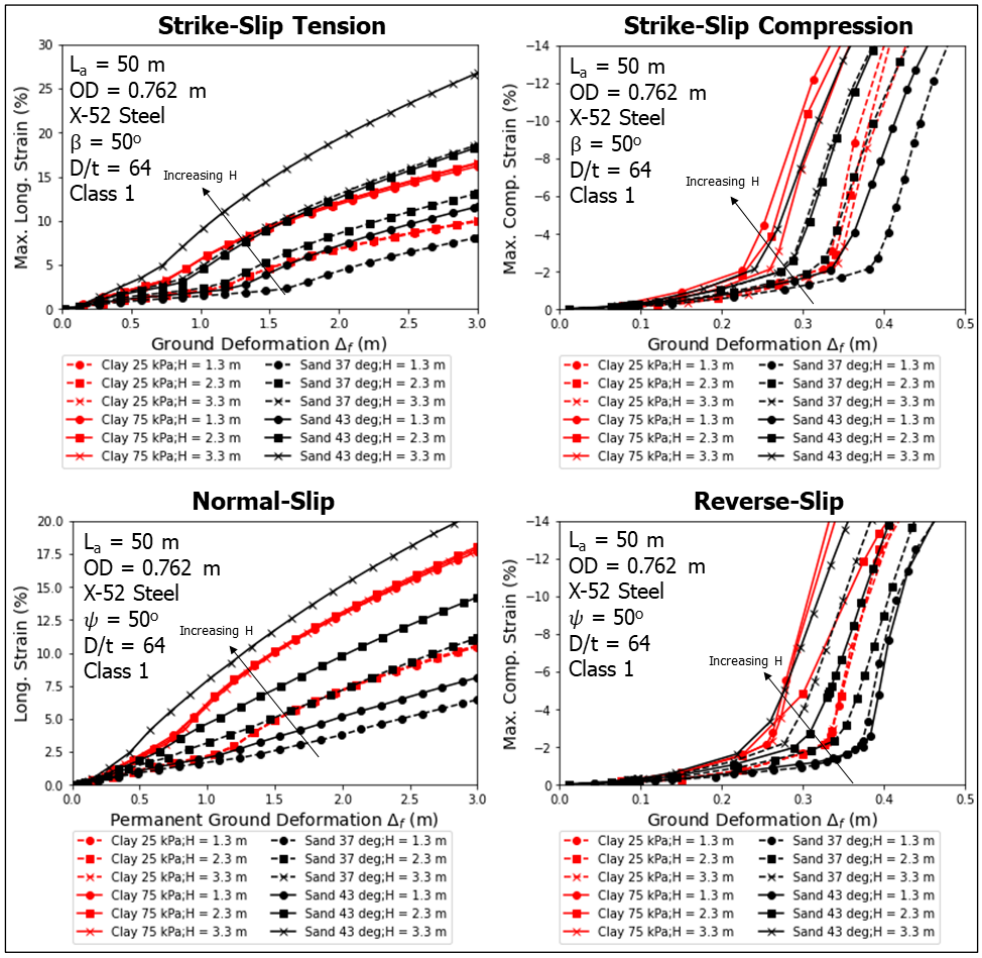

Longitudinal pipe strain versus ground deformation simulation results for soil-pipeline systems subjected to strike-slip tension, strike-slip compression, normal-slip, and reverse-slip ground deformation
Source: Bain et al. (2022)

Using the parameters found to most affect the results, more than one million numerical simulations of pipelines subjected to permanent ground deformation were performed. The simulation results were used to develop relationships that estimate a distribution of longitudinal pipe strain as a function of the soil-pipeline system parameters.

Figure 12 presents numerical results in terms of the longitudinal strain for representative tensile and compressive failure mode cases. The complete suite of pipe strain estimation models for all cases is provided in Watson-Lamprey et al. (2022).

Figure 12: Modeled Pipeline Response to Tensile and Compressive Pipe Strain

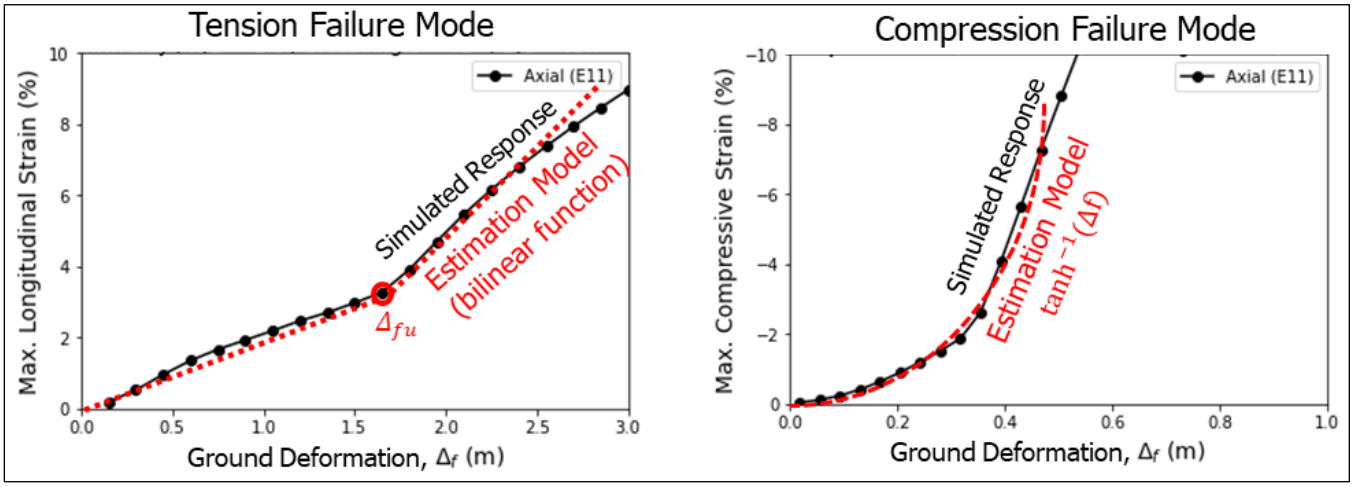

Modeled pipeline response to tensile pipe strain (strike-slip tension or normal-slip mode) and compressive pipe strain (strike-slip compression or reverse-slip mode) with examples of bi-linear and inverse hyperbolic tangent regression models used to capture the simulated responses
Source**:** Bain et al. (2022)

Wells and Caprocks

Figure 2 shows the steps within *OpenSRA* to calculate the probability of failure in wells and caprocks. The objective of this subtask is to calculate the DM by estimating a damage and fragility model for both wells and caprocks.

Fault Shear across Wells

The objective of this subtask is to assess the range of fault displacements that could result in well failure. To achieve this objective, a numerical model, using FLAC3D, was constructed to simulate the behavior of a well during fault displacement. The well comprises both the structural elements of the well and the subsurface formation that surrounds it.

Figure 13 shows the geometry and boundary conditions of the well shear model.

Figure 13: The Numerical Model for the Well Shear Simulation

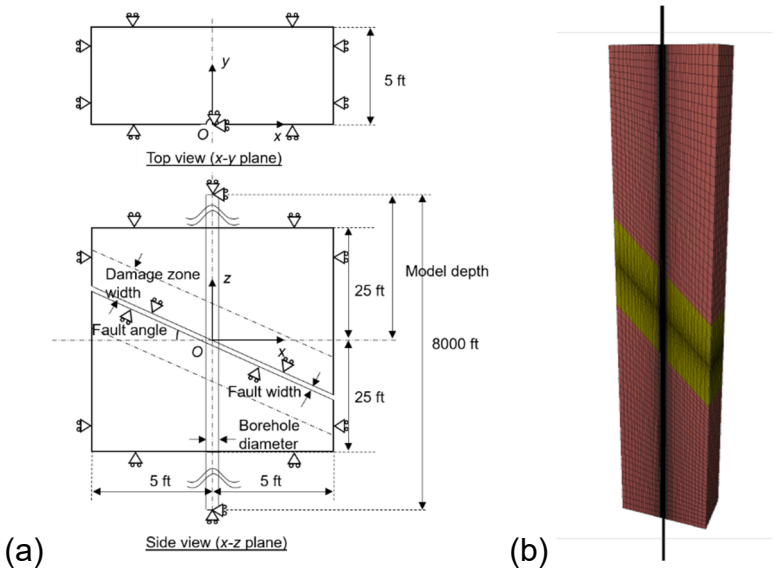

(a) The geometry and boundary conditions of the well shear model; (b) an overview of the model in FLAC3D (brown is intact rock, dark yellow fault zone)
Source: Sasaki et al. (2023)

To include the uncertainty in the depth to the top of cement, two cement scenarios were considered for each well mode, cemented and uncemented annuli. In the former case, the gap between the borehole and casing was filled with cement, whereas the latter case, the gap was left unfilled. Finally, the well shearing process was simulated by modeling reverse fault displacement as shown in

Figure 14. For further information on the materials and models used for this analysis please see Rutqvist et al. (2022). This numerical model led to both a sensitivity analysis and well fragility model more information on this can be found in the section regarding Task Group F as well as Watson-Lamprey et al. (2022).

Figure 14: Boundary Displacements and Well Shear

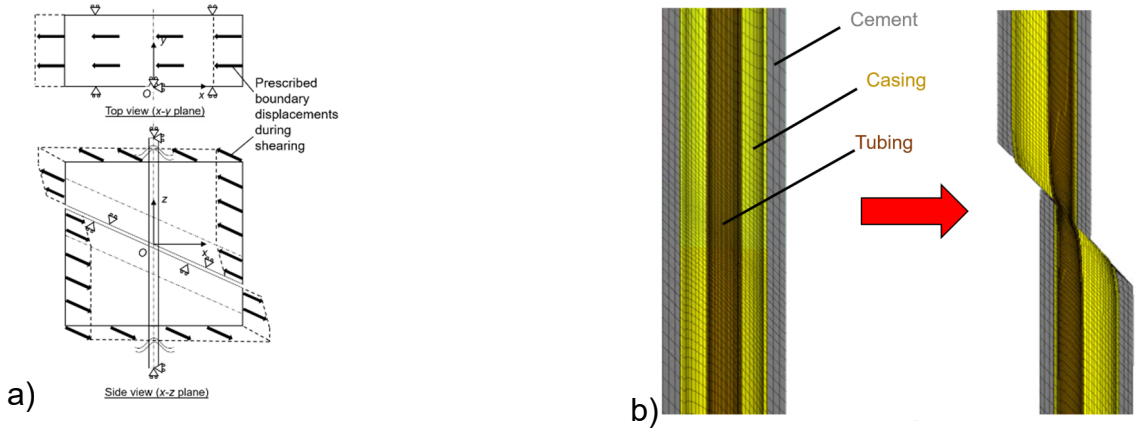

(a) Prescribed boundary displacement during shear; (b) Mesh deformation and rupture of casing and pinching of tubing during shear.
Source: Sasaki et al. (2023)

Dynamic Seismic Analysis of Well Integrity

This subtask aims to estimate the maximum bending moment a casing system can sustain when subject to earthquake-induced shaking. To do this a site-response analysis was performed using SHAKE91 to get ground motions at 2 m depth intervals. Then utilizing an open-source finite-element library OpenSeesPy v3.3 (McKenna 2011; Zhu et al., 2018) dynamic well simulations were performed. Figure 15 shows the finite-element model used for the dynamic analysis. Within this analysis maximum bending moment was used to describe the capacity of a casing system to withstand lateral loading. The results from the OpenSees model were used in a sensitivity study to develop both damage and fragility models, outlined later in this report. The details of this model can be found in Rutqvist et al. (2022).

Figure 15: Finite-Element Conceptual Model Used in OpenSees

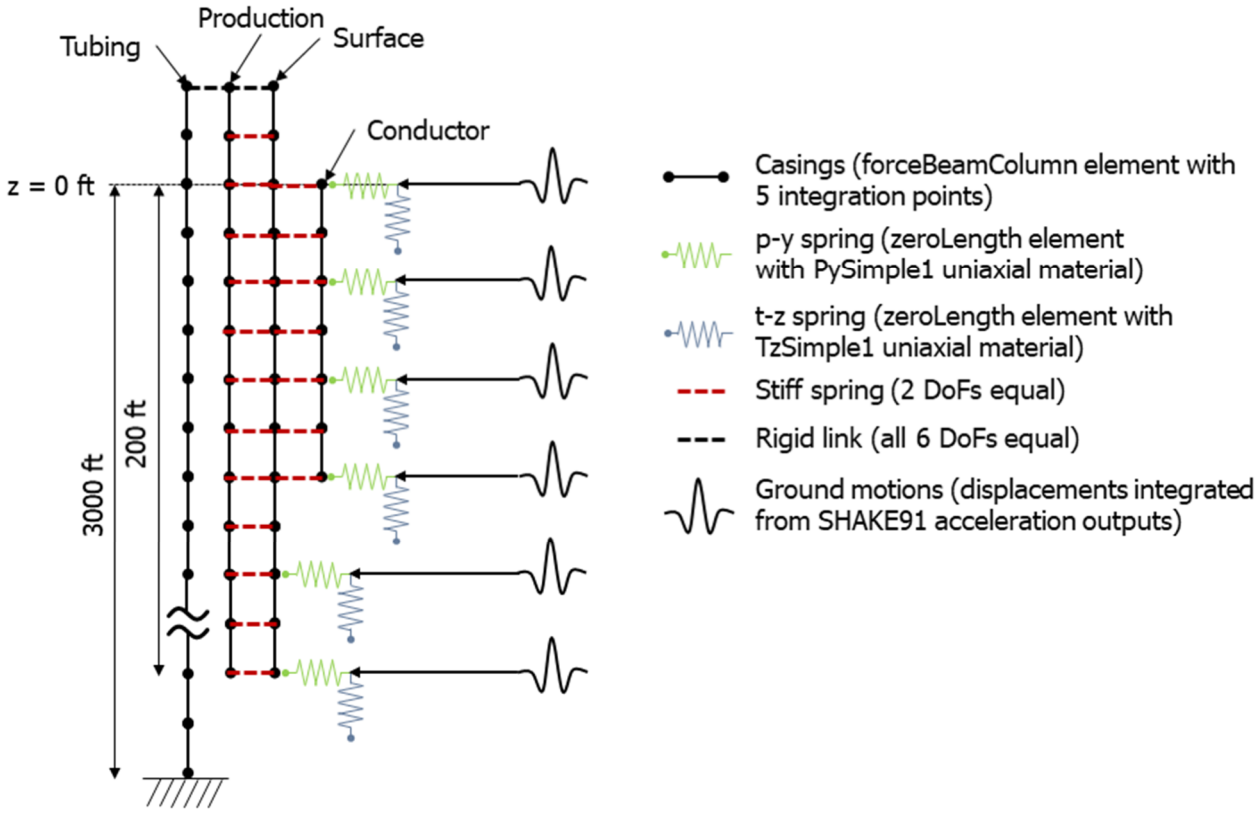

Source: Luu et al. (2023)

Caprock Integrity

In a seismic event, faults that cross a caprock could cause increased permeability if activated. This zone connects the reservoir with the formations above, creating a leakage pathway for gas to migrate upward. If the storage reservoir is also over pressured, reservoir fluid will have a driving force to migrate upwards, leading to gas loss or other environmental impacts.
This subtask first established a relationship between shear displacement and fault transmissivity; then developed a numerical model to calculate damage rates resulting from changes in fault transmissivity; assessed the depth of and pressure in a gas storage reservoir susceptible to leakage; and finally performed a suite of simulations that capture uncertainties to calculate the overall fragility of caprocks (see Rutqvist et al. (2022) for additional information regarding the literature review, statistics on caprocks, etc.).

For the numerical modelling TOUGH (Transport of Unsaturated Groundwater and Heat) program was used through iTOUGH2 (inverse TOUGH2). Most of the UGS reservoirs in California are operated far below the hydrostatic pressure (Zhang et al., 2023). Even when caprock integrity is compromised due to an earthquake, gas may not leak out due to the lack of a driving force. Kirby Hills Domengine storage facility was found to be an exception. As such the parameters from this storage facility were adapted in the numerical model. A schematic of the model is shown in Figure 16. Four scenarios for this model are considered in the next step to drive the fragility curve:

- Both the UGS reservoir and the formation above the caprock have open boundaries;
- Both the UGS reservoir and the formation above the caprock have closed boundaries;
- The UGS reservoir has open boundaries and the formation above the caprock has closed boundaries;
- The UGS reservoir has closed boundaries and the formation above the caprock has open boundaries.

The model output is the cumulative gas leakage over time and led to the fragility model described later in this report.

Figure 16: The Schematics of the Numerical Model for Calculating Fault Leakage

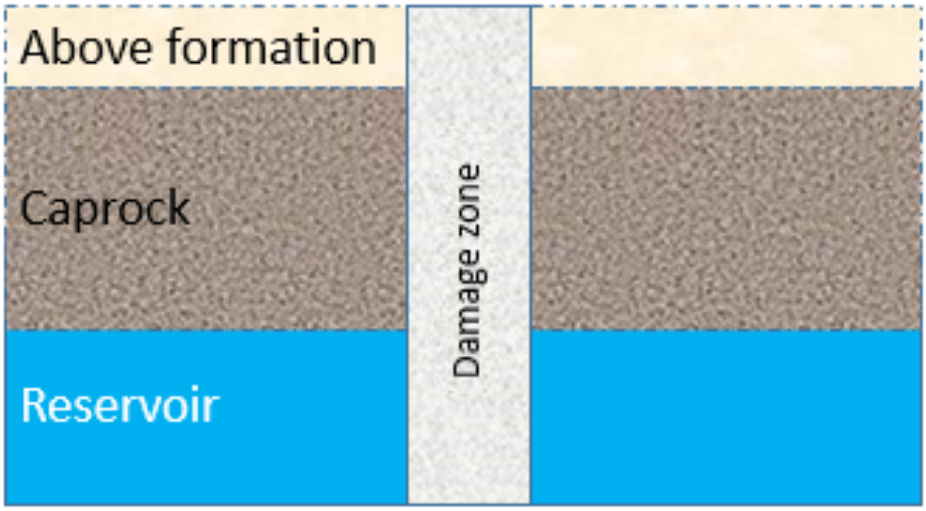

Not to scale.
Source: Zhang et al. (2023)

Aboveground Infrastructure
This subtask focused on developing fragility curves for different components of surficial infrastructure (see Figure 3). The analyses in this task are split into five outcomes:

- Outcome #1: Experimental Data on Critical Components
- Outcome #2: Experimental Data Relative to Subsystems
- Outcome #3: Calibrated Nonlinear Steel Properties
- Outcome #4: Seismic Analysis of Nonlinear Subsystems
- Outcome #5: Fragility Development

Outcome #1: Experimental Data on Critical Components

Table 6 presents the test matrix for the component tests performed at the Powell laboratories at the University of California, San Diego. Because these components behave differently depending on the direction of loading, select components were tested in the in-plane and out-of-plane direction.

Table 6: Test matrix of component specimens (Pantoli et al. 2022)

Component type	Diameter (Schedule)	Direction of loading	Short name
Tee	4 in (80)	In-plane	4T-IP
	4 in (80)	Out-of-plane	4T-OP
	8 in (40)	In-plane	8T-IP
	8 in (40)	Out-of-plane	8T-OP
90° elbow	4 in (80)	In-plane	4E-90
45° elbow	4 in (80)	In-plane	4E-45

Pre-test simulations were performed using Abaqus, for each specimen, to support the development of the load protocol and instrumentation plans. Figure 17b shows an example of the meshed model of a specimen in Abaqus. For specifics on material type and model development see Pantoli et al. (2022). Photograph, (b) Modeled and meshed in Abaqus

Source : Pantoli et al. (2022)

Figure 18 through
Source: Pantoli et al. (2022)

Figure 20 show the test set up for the individual components and their corresponding schematic.

Figure 17: Specimen 4T-OP

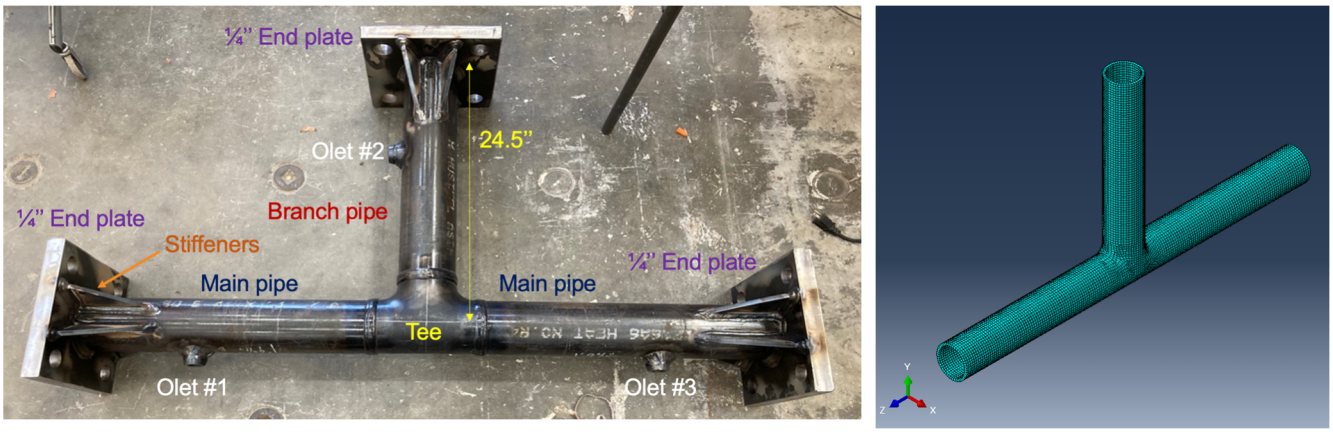

(a) **(b)**

(a) Photograph, (b) Modeled and meshed in Abaqus
Source : Pantoli et al. (2022)

Figure 18 : Specimen 8T-IP

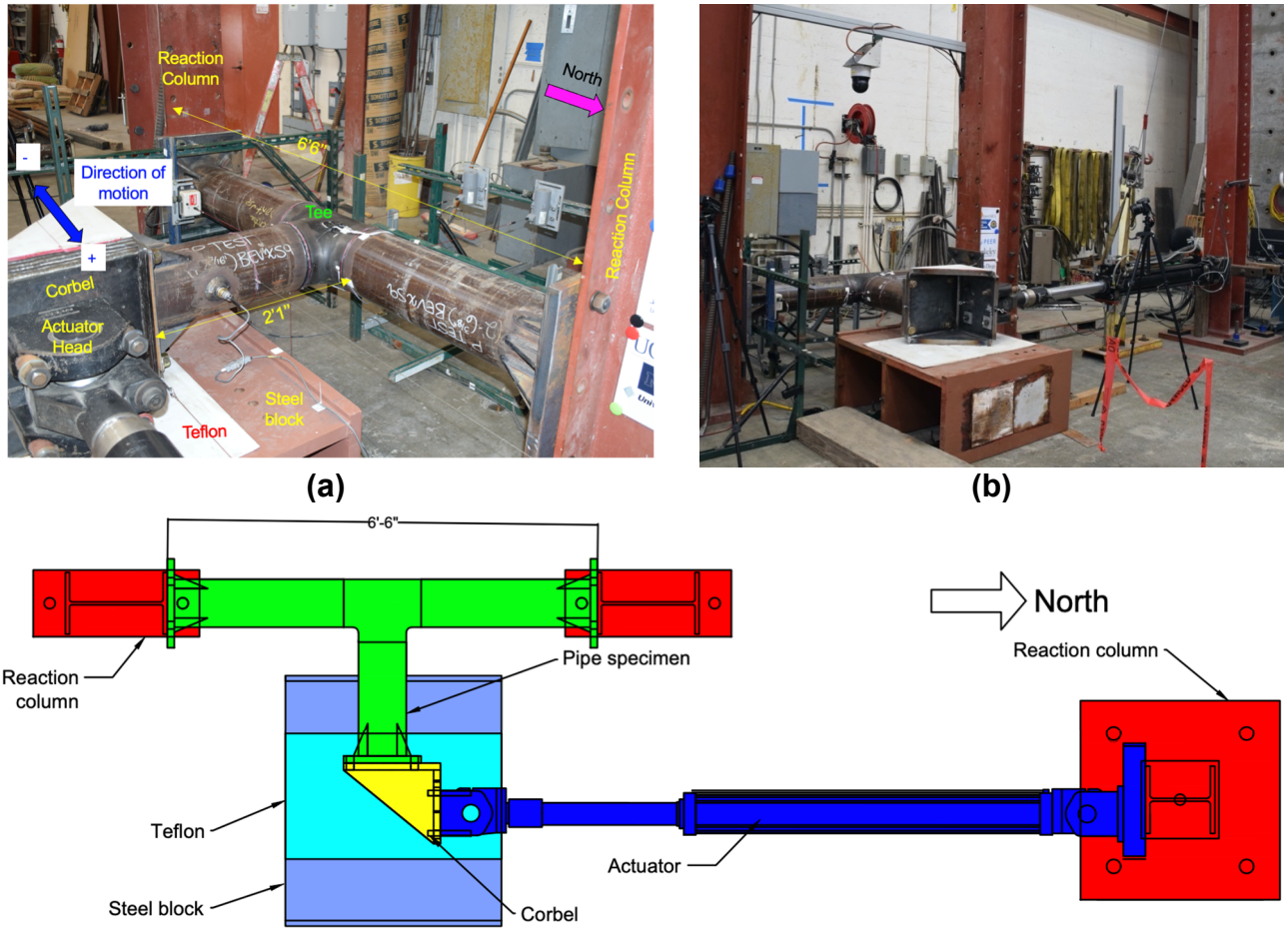

(a), (b) Photographs, (c) Plan view

Source: Pantoli et al. (2022)

Figure 19: Specimen 4T-OP

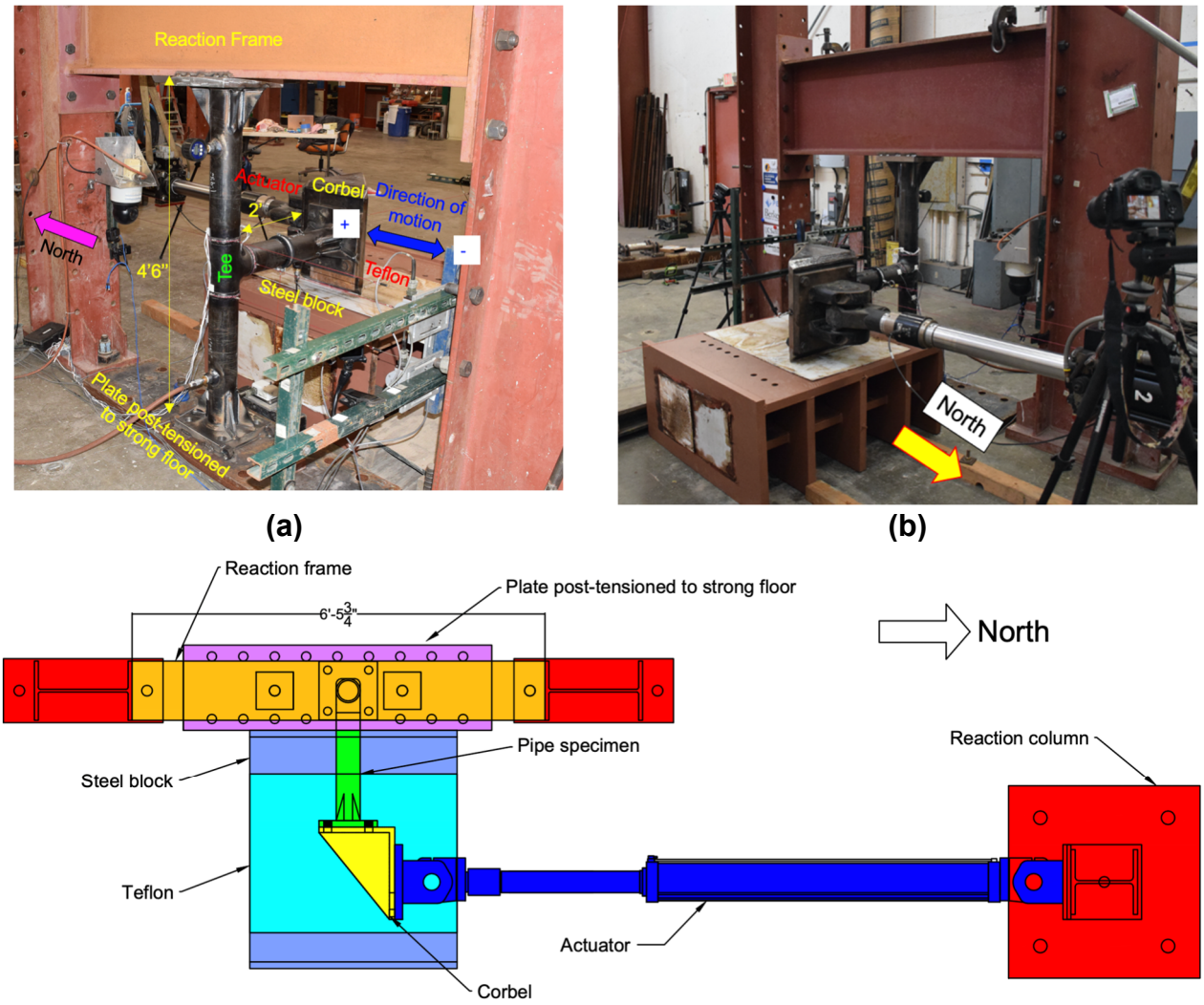

(a), (b) Photographs, (c) Plan view
Source: Pantoli et al. (2022)

Figure 20: Specimen 4E-90

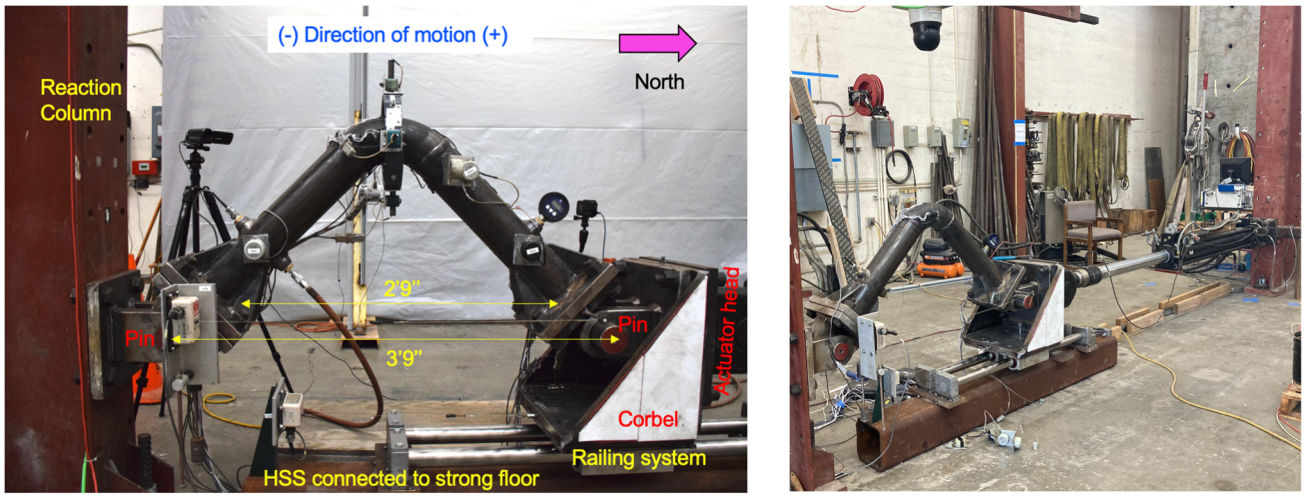

(a)

(b)

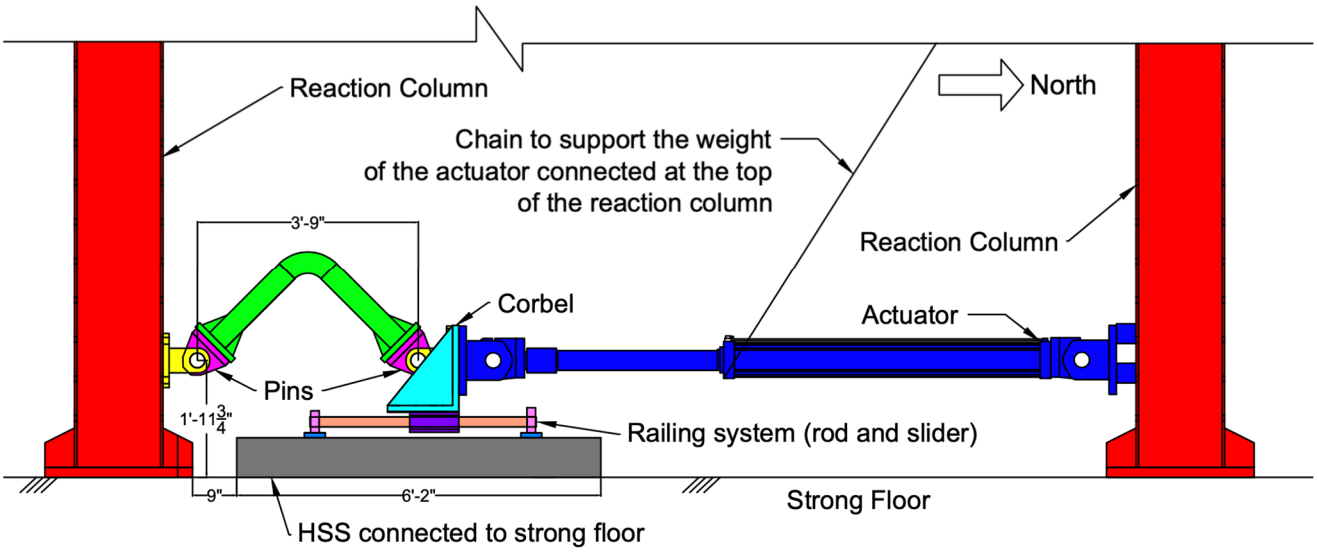

(c)

(a), (b) Photographs, (c) Plan view
Source: Pantoli et al. (2022)

The progression of damage was the same for all the specimens except 8T-IP, and included the following limit states:

1. First ovalization. This limit state identifies the moment when a visible deformation of the component could be observed for the first time.
2. First crack. This limit states indicate the appearance of a shallow crack at locations of high strains.
3. Through crack. Sudden loss of internal pressure happened when the continuous displacement applied to the specimen lead one or more shallow cracks to become through cracks. This is considered the “failure” of the specimen.

Components failing in this way are deemed “ductile”, since they show warning signs before failure happens. The only specimen that had a “brittle” failure far from the location of high strains predicted by Abaqus was 8T-IP.

Outcome #2: Experimental Data Relative to Subsystems

A dynamic test series was conducted on a generic (full-scale) surface infrastructure subsystem at the Earthquake Engineering Laboratory at UNR using two biaxial shake tables. Figure 21 shows a rendering of the subsystem tested at UNR while

Source: Pantoli et al. (2022)

Figure 22 shows a photograph of this subsystem and its relevant components.

Figure 21: Rendering of the subsystem experiment

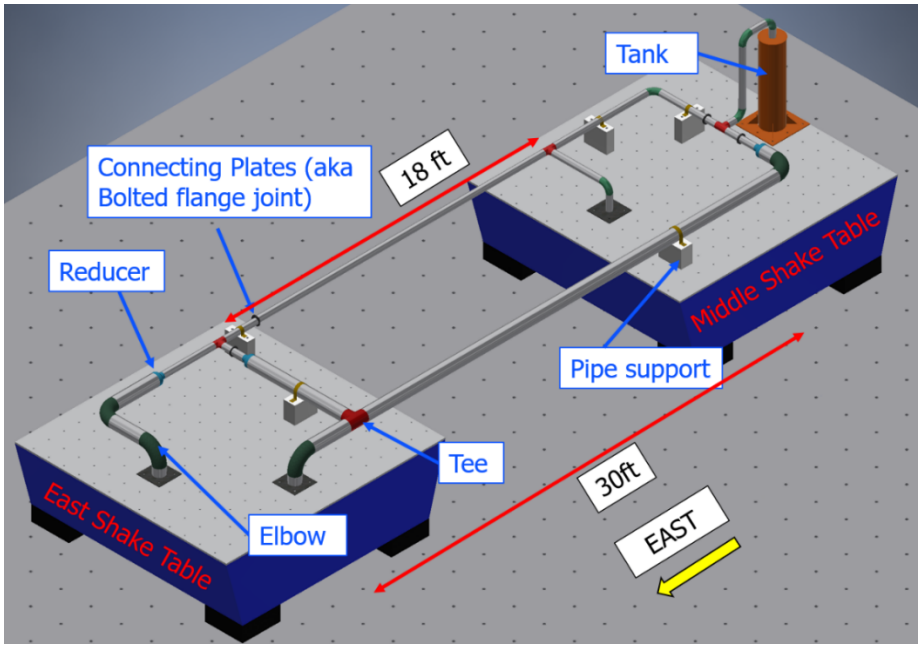

Source: Pantoli et al. (2022)

Figure 22: Photograph of the subsystem tested at UNR

(a)

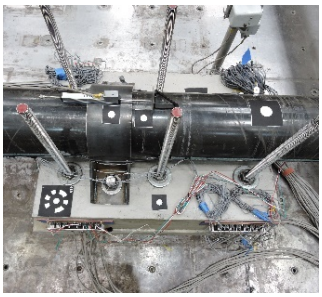

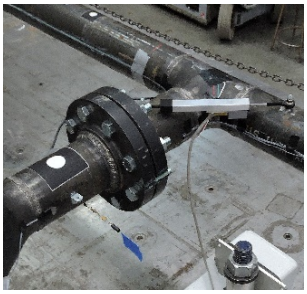

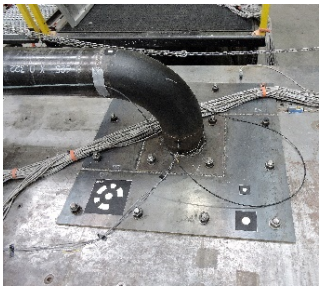

(b)(c) **(d)(e)** **d)** **(e)**

(a) Assembled subsystem on the UNR shake tables, (b) Pipe support, (c) Connecting plates, (d) Elbow , (e) Vertical tank.

Source: Pantoli et al. (2022)

A nonlinear numerical model was developed before the test to gain insights on the expected behavior of the subsystem. This model was developed using OpenSees and is shown in

Figure 23. Information on the validation of this model can be found in Pantoli et al. (2022). The model indicated no damage should occur if the subsystem was subjected to uniform earthquake accelerations, however, significant deformation and yielding could occur if the subsystem was subjected to large relative displacement. Thus, the subsystem was subjected to three types of motions. Figure 24 shows the subsystem during testing. These motions included: broad-band white noise, synchronous motions, and asynchronous (time shifted) motions.
Source: Pantoli et al. (2022)

Figure 25 presents an example of asynchronous time motion. Information on the test setup, instrumentation and loading protocol are provided by Elfass et al. (2023).

Figure 23: Plan view of pre-test model in OpenSees

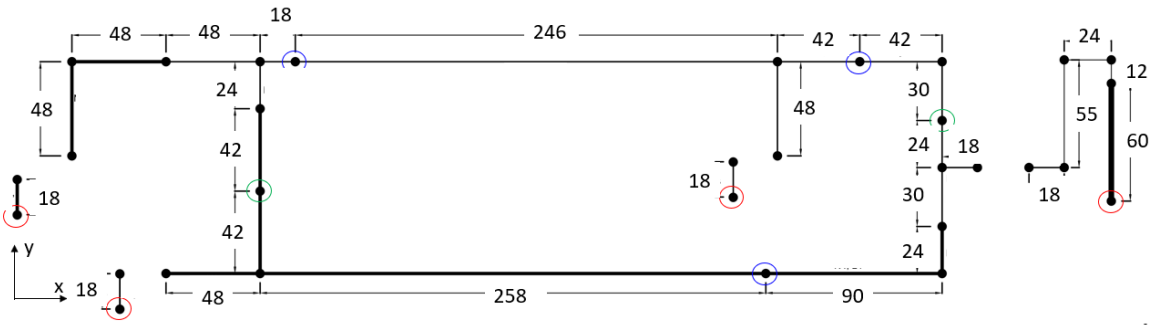

All dimensions in inches. Red circles denote fixed supports in all degrees of freedom, green circles denote restrained supports in X and Z directions, blue circles denote restrained supports in Y and Z directions.

Source: Pantoli et al. (2022)

Figure 24: Views from two high-resolution cameras

(a) **(b)**

(a) Top view, (b) Side view

Source: Pantoli et al. (2022)

Figure 25: Time history of the asynchronous motions

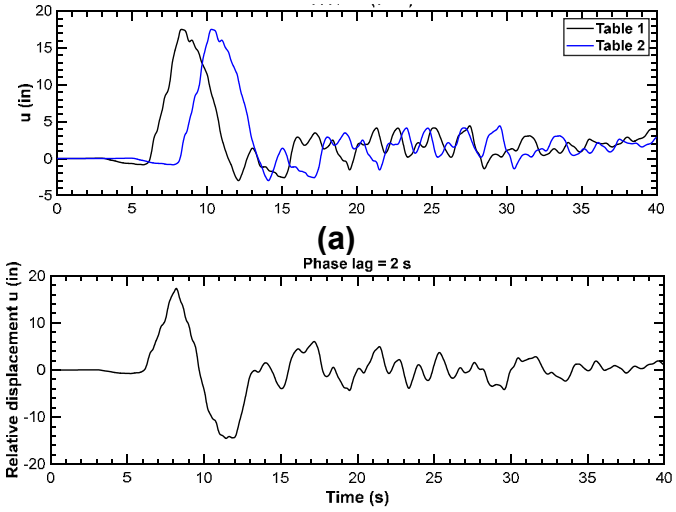

(a) Displacement time history for each shake table, (b) Time history of the resulting relative displacement between shake tables

Source: Pantoli et al. (2022)

Through these laboratory tests it was found that only the large relative deformations caused any yielding or failure.

Figure 26 shows the progression of the behavior at relative displacements of 17 inches. The red dots denote where yielding occurred, and the number represents the ratio between the maximum strain measured at that location at the yield strain. It was also noted that the subsystem did not experience any leaks or loss of pressure.
Source: Pantoli et al. (2022)

Figure 27 provides pictures of pipe deformations showing the rotation experienced by both pipelines. However, at such rotation, damage was observed to the concrete pedestal at one pipe support, as shown in
Source: Pantoli et al. (2022)

Figure 28.

Figure 26: Observed yielding at two cycles of 17 in of shake table relative displacement

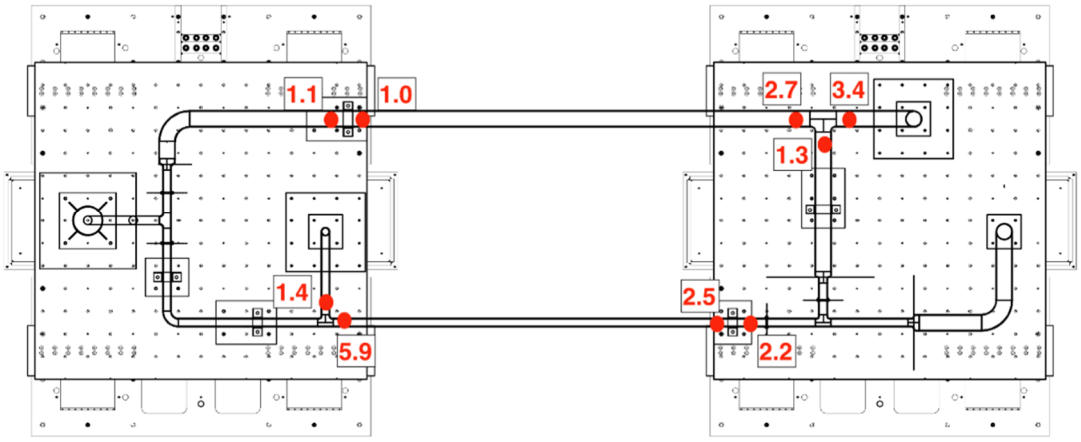

Source: Pantoli et al. (2022)

Figure 27: Piping deformation at 17 in of relative shake table displacement

(a)

(b)

(a) North table moving east, (b) North table moving west
Source: Pantoli et al. (2022)

Figure 28: Damage at a pipe support after the final motion

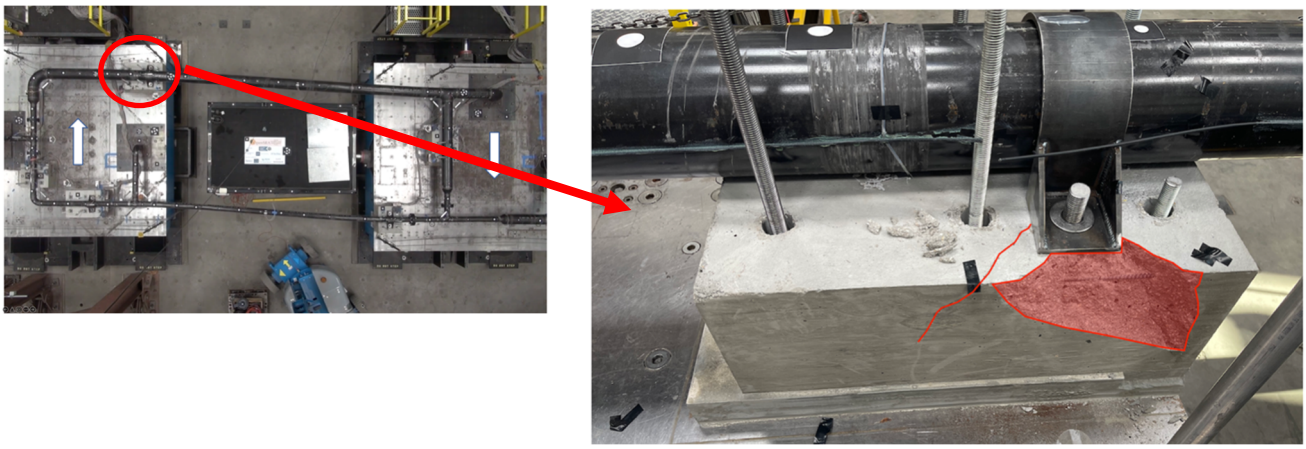

Source: Pantoli et al. (2022)

Outcome #3: Calibrated Nonlinear Steel Properties

Creating a robust and reliable nonlinear material model for steel is required for the reasonable prediction of the behavior of a steel component subjected to the large cyclic deformations that

can be caused by earthquakes. To support this need, the aforementioned component experimental data were utilized in iterative form to calibrate the nonlinear material properties for the steel used for tees and elbows in the finite element models.

The optimal values of the cyclic hardening parameters were obtained by minimizing the error between the experimental results from component tests and the corresponding Abaqus numerical predictions for all specimens tested. Figure 29 and Figure 30 show example results of the calibration of these materials using a comparison of experimental and numerical results. Further information about the validation process can be found in Pantoli et al. (2022).

Figure 29: Comparison of numerical and experimental moment-rotation curves

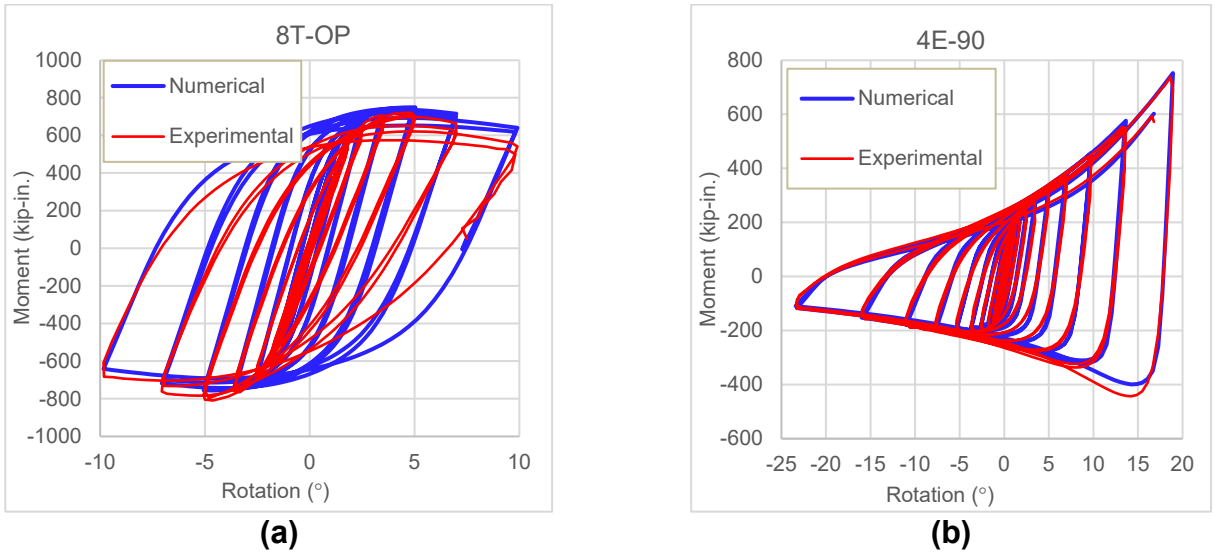

(a) **(b)**

(a) Specimen 8T-IP, (b) Specimen 4E-90
Source: Pantoli et al. (2022)

Figure 30: Comparison of numerical and experimental time history of moment

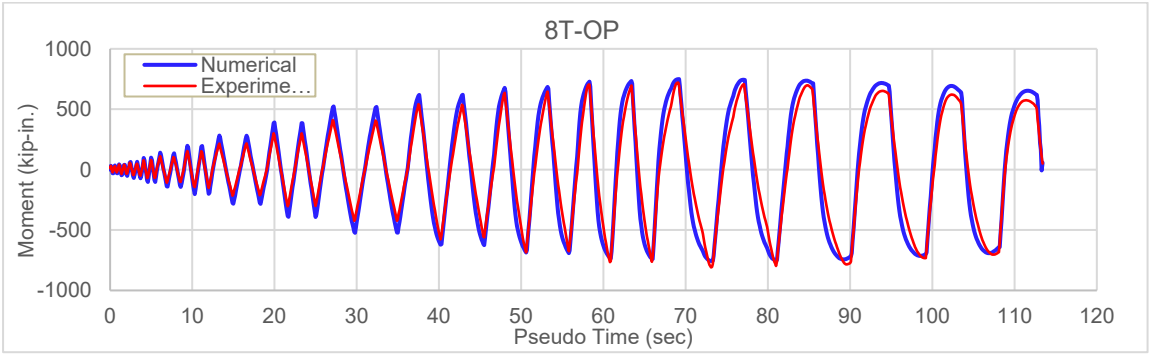

(a)

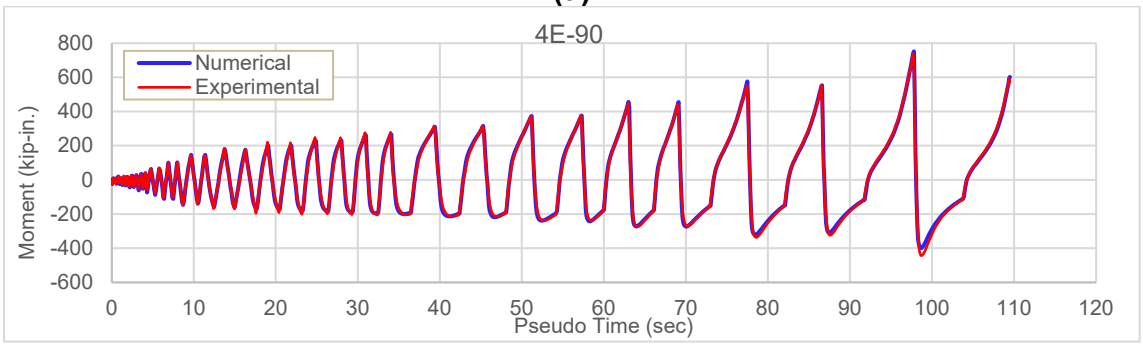

(b)

(a) Specimen 8T-IP, (b) Specimen 4E-90
Source: Pantoli et al. (2022)

Outcome #4: Seismic Analysis of Nonlinear Subsystems

Task Group D developed a procedure for the seismic analysis of nonlinear gas subsystems using OpenSees which can be used to generate fragility curves for *OpenSRA*. In this procedure, the nonlinearities and failure points of the subsystem are concentrated at the location of critical components, while the remainder of the model subsystem remains linear. The subsystems explored are the wellhead tree-pipeline (WTP) subsystem where buried pipelines come to the surface and end in a wellhead, that then distributes the gas aboveground, and vertical pressure vessels (VPV). The geometry of these subsystems is based on photographic evidence found on public resources, design calculations, manufacturer catalogues of valves and other components, site visits to a gas storage facility, and personal communication with experts at utility companies.

WTP Subsystem

A typical wellhead tree is depicted in **Error! Reference source not found.**a and the corresponding OpenSees model used for fragility development is shown in **Error! Reference source not found.**b. Further information regarding wellhead trees and their geometry in California and Validation of the OpenSees model can be found in Pantoli et al. (2022).

Figure 31: Wellhead tree

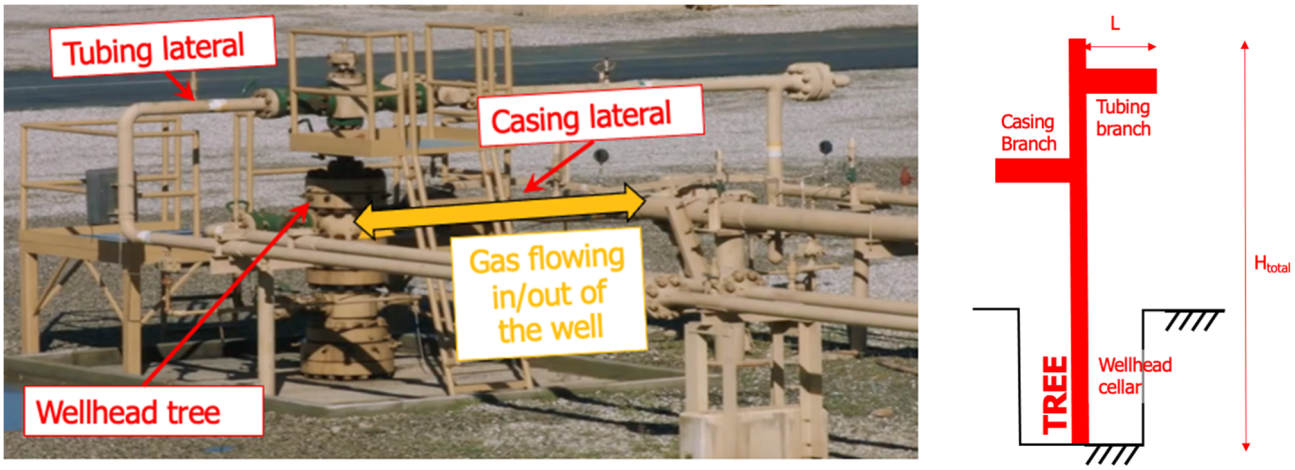

(a) Photograph of a wellhead tree and connected piping, (b) Schematic of a wellhead tree showing relevant nomenclature

Source: Edited from SoCalGas (2016)

The procedure used to calibrate the parameters of this model in OpenSees involved the following:

- A numerical model of the critical components and sections of straight pipes created in Abaqus. This model uses the calibrated material properties obtained in outcome #3 and the field boundary conditions. The Abaqus model of the tee rotating in-plane is shown in Figure 32a.
- An OpenSees model of the same geometry and boundary conditions is created, as shown in Figure 32b.
- The two models are subjected to the same displacement-controlled cyclic analysis with a load protocol
- The forces necessary to obtain this displacement in the Abaqus and OpenSees are compared

This same procedure can be used to extend the results to a wider range of component types/details and loading conditions. As an additional step in validation, impact tests were performed at a gas storage field in California, additional information on these tests can be found in Pantoli et al. (2022).

Figure 32: Component models for the tee rotating in-plane

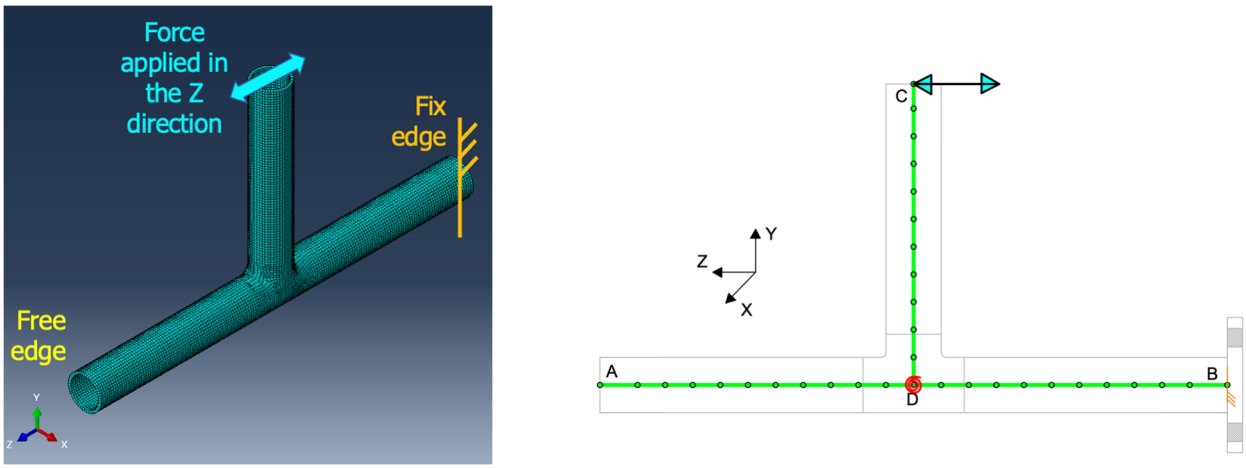

(a) **(b)**

(a) Abaqus model, (b) OpenSees model
Source: Pantoli et al. (2022)

VPV Subsystem

The vertical pressure vessels observed at gas storage facilities comprise a tall cylindrical vessel with hemispherical or elliptical heads supported by a skirt (Figure 33a). The optimal EDP for these analyses is the ratio between the moment demand at the base imposed by an earthquake and the moment capacity at which a limit state is achieved.

Validation of the VPV Subsystem

For the validation of this subsystem, a sample VPV geometry was selected based on representative information of a pressure vessel provided by a gas company in California. This sample VPV was modeled using Abaqus and complimentary but simplified linear version utilizing 1D finite elements within OpenSees. These results show that:

- The movement of the pressure vessel itself is not affected by the movement of the pipes.
- The inlet pipe connected to the bottom of the pressure vessels has minimal movement in these lower frequency modes.
- The simplified OpenSees model can capture the behavior of this subsystem predicted by the more refined Abaqus model.

Figure 33: Vertical pressure vessels

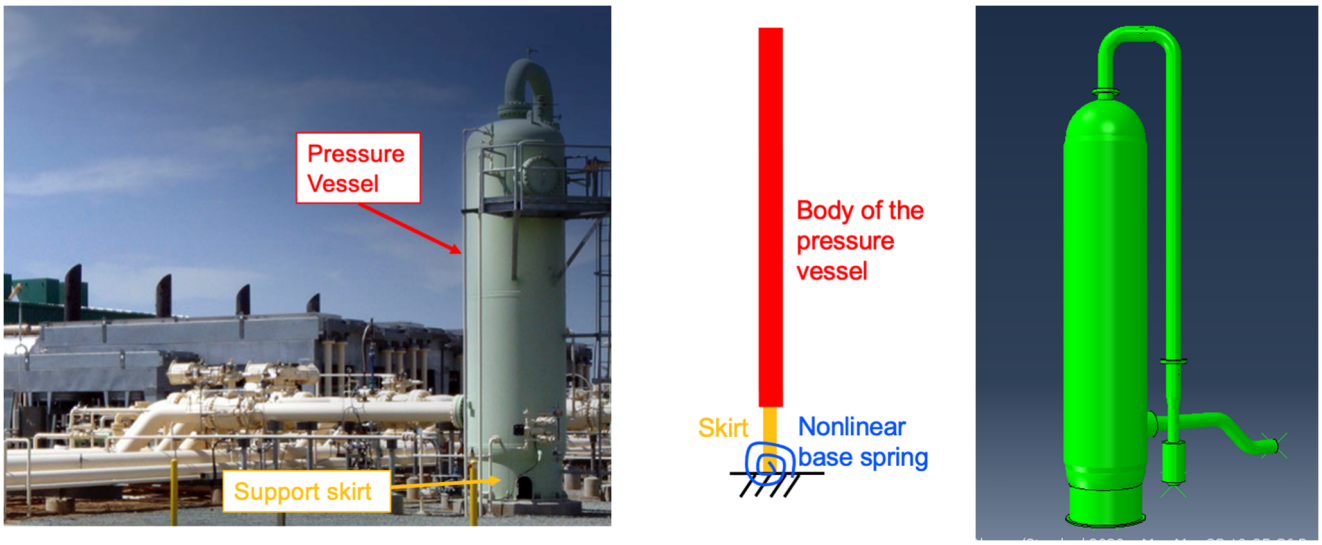

(a) Photograph (RockPoint Gas Storage 2021), (b) Schematic of the OpenSees Model, (c) Abaqus model
Source: Pantoli et al. (2022)

Outcome #5 – Damage Models

The final fragility functions developed for outcome #5 are fully presented in Watson-Lamprey et al. (2022). The following includes a sample of the damage model curves developed for 4T-IP at no pressure and high pressure are presented in blue and orange in Figure 34. The polynomial curves were obtained interpolating the relevant points.

Figure 34: DM(EDP) curves for 4T-IP

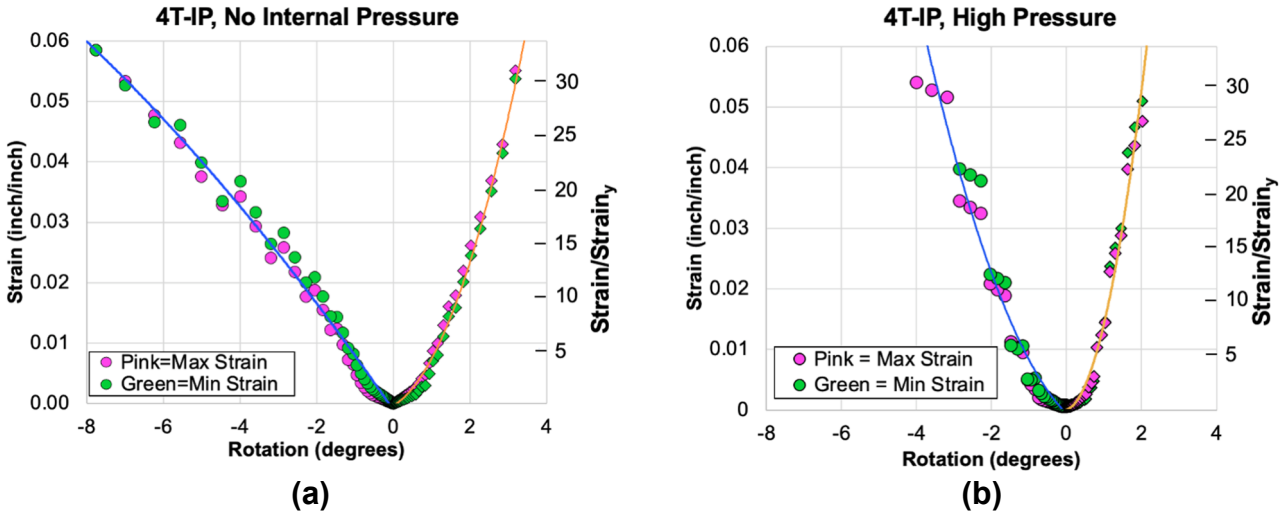

(a) No internal pressure, (b) High internal pressure
Source: Pantoli et al. (2022)

Task E – Sensing Technologies
The goal of this task is to identify the technologies that can inform the risk models at the input, intermediate, and final output stages.

The sensing technologies introduced in Wang et al. (2021) were selected depending on *OpenSRA* parameters, which include geologic information and characteristics of the gas infrastructure. The selected sensing technologies can be categorized into four main categories:

1. Remote sensing technologies
2. Continuous monitoring technologies
3. Inspection technologies
4. Leakage detection technologies

Remote Sensing Technologies
Ground deformation is an important input in *OpenSRA* regardless of the level of analysis. Remote sensing technologies have been used widely to detect and monitor objects (including ground deformation). Table 7 presents a comparison of these technologies and their uses.

Table 7: Comparisons of Remote Sensing Technologies (Wang et al. 2021)

TECHNOLOGY	ADVANTAGES	DISADVANTAGES	OCCASIONS
LiDAR	Highest accuracy, able to penetrate vegetation	Cannot penetrate fog and rain, high cost	Most cases except during fog or rain
InSAR	Accurate, available for most cases	High cost	Most cases
Aerial and satellite photography	Relatively low cost	Need line of sight	Low-vegetation area or vegetation height is considered, and without fog and rain

Continuous Monitoring Technologies
Continuous monitoring technologies are deployed on site and operate on stand-alone power and cellular communication. The selected continuous monitoring technologies include distributed fiber optic sensors (DFOS) and wireless sensor network (WSN).

Table 8 and Figure 35 specifically outline uses of WSN and mor information regarding DFOS and the tests done within this project can be found in Wang et al. (2021).

Table 8: Wireless Sensor Network Based Sensing Technologies and the Corresponding Events and Occasions (Wang et al. 2021)

TECHNOLOGIES	EVENTS	OCCASIONS
Soil moisture sensor	Leakage	Underground pipeline
Accelerometer	Leakage	All
Strain gauge	Deformation	All
Position sensor	Relative displacement	Aboveground pipeline
*Flow sensor	Leakage	All
*Gas sensor	Leakage	Mostly aboveground

Figure 35: WSN Instrumentations

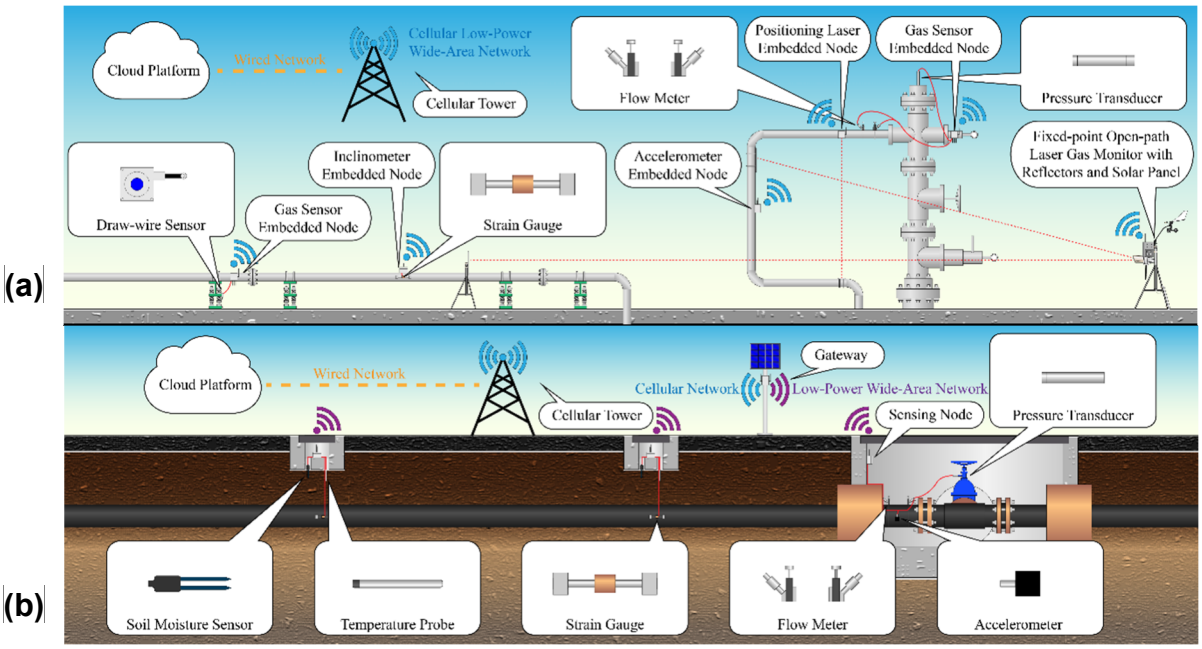

(a) Aboveground (b) Underground Gas Pipeline Monitoring
Source: Wang et al. 2021

In-line Inspection Technologies

Inspection technologies specifically help identify pipeline characteristics from inside the pipe. These characteristics can be used as a reference for inputs and to verify the intermediate and final outputs of *OpenSRA*. This project focused on the In-line Inspection (ILI) techniques which can be done at the same time with the periodically pigging progress. Table 9 compares different ILI technologies and their applications.

Table 9: Associable Sensing Technologies for Smart PIG (Wang et al. 2021)

TECHNOLOGY	APPLICATION
Magnetic Flux Leakage (MFL)	Surface pitting, corrosion, cracks and weld defects detection (for steel/ferrous pipelines only)
Ultrasonic	Cracks, coating and lamination defects detection
Caliper	Bending and other deformations
Temperature Sensor	Providing the indication of the likely type of debris present
Odometer	Providing the travel distance of the pig
Orientation Sensor	Providing the travel direction of the pig
Vibration Sensor	Providing position fixing at each joint

Leakage Detection Technologies

Gas and flow sensing technologies help characterize leakage events and provide information on the amount of the leakage. This helps utility owners focus mitigation efforts after a seismic event occurs. This project introduces different types of gas and flow sensors, including their

mechanisms, abilities, limitations, and comparisons as a reference for helping users to select the sensors that suit their applications best (Table 10).

Table 10: Comparison of Gas Flow Monitoring Technologies (Wang et al. 2021)

TECHNOLOGY	ADVANTAGES	DISADVANTAGES	OCCASIONS
Coriolis	High accuracy and turndown ratio, independent of fluid properties and entrained gases	Expensive to purchase and install, pressure drop, not suitable for large pipe size	Small pipe sizes, changing conditions
Thermal mass	High accuracy and repeatability, easy to install	Very low response time, dry and clean fluids	Dry and clean fluids
Turbine	Very high versatility and accuracy, fast response time, high pressure and temperature capabilities	Moving parts can wear or clogged, not suitable for low flow rate	Not for low flow, viscous, dirty and corrosive fluids
Ultrasonic	Very high versatility and accuracy, no pressure drop, low maintenance, non-invasive	Expensive, not suitable for low flow rate	Not for low flow
Vortex	Low pressure drop, High versatility and pressure capability	Limited by viscosity and minimum flow rate, need temperature and pressure compensation, no entrained solid and gas	Clean gas, high pressure, low viscous fluids
Differential pressure	Flexible specification, experienced and reliable, generally low cost	Limited range ability, complex installation	Most occasions
Positive displacement	Very high versatility, accuracy and turndown ratio, reliable	Moving parts can wear or clogged, need temperature and pressure compensation, pressure drop	Most occasions (includes viscous, dirty and corrosive fluids)

OpenSRA Informing Technologies Guidance

Measured data (as seen in the laboratory testing in previous sections) aids in the industry's understanding of how a system reacts specifically in a seismic event. Leveraging this measured data will continue the progress made in this project to update current risk models. Implementing sensing technologies now will aid the industry in decision-making and risk mitigation in the future. The following tables outline how different sensing technologies can better the analyses on specific gas infrastructure.

Gas Pipelines

The pipeline response estimate requires both infrastructure and geotechnical characteristics. Table 11 shows examples of the required input as well as intermediate, and final output parameters used with this tool.

Table 11: Gas Pipeline Simulation Tool Parameters (Wang et al. 2021)

VARIABLES		DESCRIPTION	UNIT	AVAILABLE TECH
INPUT	STRUCTURAL	Pipe outside diameter	mm	Ultrasonic, Magnetic Flux Leakage with caliper
		Pipe wall thickness	mm	Ultrasonic, Magnetic Flux Leakage
		Pipe yield stress	kPa	-
		Ramberg-Osgood parameter	UNIT-LESS	-
		Ramberg-Osgood parameter	UNIT-LESS	-
	GEOTECHNICAL	Total unit weight of backfill soil	kN/m^3	-
		Soil cover to centerline of pipeline	m	-
		Length of ground deformation zone	m	LIDAR
		Backfill friction angle	Degree °	-
		Sand/pipe interface friction angle ratio	UNIT-LESS	-
		Permanent ground deformation	m	LIDAR, InSAR, Structure from Motion
INTERMEDIATE		Force per unit length of pipeline	kN	DSS, WSN (Strain gauge)
		Pipe burial parameter	kPa	-
		Embedment length	m	-
		Standard deviation of L_e estimate (ln units)	-	-
		Value of L to use in pipe strain equation	-	-
OUTPUT		Pipe strain	%	DSS, WSN (Strain gauge)
		Standard deviation of pipe strain estimate (ln units)	-	-
		Epistemic uncertainty	-	-

All variables and references used for description in this table correspond to Task B report

Gas Storage Wells

Both the well characteristics and ground conditions are required by the gas storage wells response estimate.

Table 12 shows examples of the required input, generated intermediate and final output parameters used in this tool.

Table 12: Gas Storage Wells Simulation Tool Parameters (Wang et al. 2021)

VARIABLES		DESCRIPTION	UNIT	AVAILABLE TECH
INPUT	CASING & TUBING	Casing-tubing interface friction coefficient	-	-
		Casing Pressure	MPa	WSN (pressure sensor)
		Young's modulus of casing/tubing	GPa	-
		Density of casing/tubing	kg/m^3	-
		Poisson's ratio of casing/tubing	-	
		Internal friction angle of cement	Degree °	-
		Uniaxial compressive strength of cement	MPa	-
		Tensile strength of cement	MPa	-
		Yield strength of casing/tubing	Ksi	-
		Yield/Tensile strength ratio of casing/ tubing	-	-
	WELLHEAD	Wellhead mass per length	kg/m [lb/in]	-
		Wellhead height	m [ft]	LIDAR, Structure from Motion, WSN (displacement)
	GEOTECHNICAL	Fault angle	Degree °	-
		Fault core width	m	-
		Damage zone width	m	-
		Depth of fault-well intersection	m	-
		Maximum horizontal-to-vertical effective stress ratio	-	-

VARIABLES		DESCRIPTION	UNIT	AVAILABLE TECH
		Young's modulus of rock	GPa	-
		Density of rock	kN/m^3	-
		Permanent ground deformation	m	LIDAR, InSAR, Structure from Motion
INTERM-EDIATE		Fault Displacement	m	LIDAR, InSAR, Structure from Motion
OUTPUT		Pipe strain	%	DSS, WSN (Strain gauge)
		Pipe bending moment	kN-m [lbs-ft]	DSS, DAS
		Standard deviation of pipe strain estimate (ln units)	-	-
		Epistemic uncertainty	-	-

All variables and references used for description in this table correspond to Task C report

Aboveground Gas Infrastructure

The infrastructure response estimate requires the characteristics of the target infrastructural components, which include pipes, elbows, tee joints, vessels, outlet and inlet pipes. Table 13 shows examples of the required input and generated final output parameters used in this tool.

Table 13: Aboveground Gas Infrastructure Simulation Tool Parameters (Wang et al. 2021)

VARIABLES		DESCRIPTION	UNIT	AVAILABLE TECH
INPUT	-	Pipe yield stress	MPa [psi]	-
	PIPES	Outside diameter of the pipeline.	mm [inch]	LIDAR, Ultrasonic, Magnetic Flux Leakage with caliper
		Wall thickness of the pipeline.	mm [inch]	Ultrasonic, Magnetic Flux Leakage
	ELBOWS	Outside diameter of the pipeline.	mm [inch]	LIDAR, Ultrasonic, Magnetic Flux Leakage with caliper
		Wall thickness of the elbows.	mm [inch]	Ultrasonic, Magnetic Flux Leakage
	TEES	Outside diameter of the tees.	mm [inch]	LIDAR, Ultrasonic, Magnetic Flux Leakage with caliper
		Wall thickness of the tees.	mm [inch]	Ultrasonic, Magnetic Flux Leakage
	VESSEL	Total height of the pressure vessel.	m [ft]	LIDAR, Structure from Motion, WSN (displacement)
		Diameter of the pressure vessel.	-	LIDAR, Structure from Motion
		Design pressure for the vessel (used to calculate thickness).	-	-
		Vessel thickness.	mm [inch]	Ultrasonic, Magnetic Flux Leakage
	OUTLET PIPE	Height of joint 1 of outlet pipe.	%	LIDAR, Structure from Motion, WSN (displacement)
		Length of segment LO12.	%	LIDAR, Structure from Motion, WSN (displacement), DSS
		Length of segment LO23.	%	LIDAR, Structure from Motion, WSN (displacement), DSS

VARIABLES		DESCRIPTION	UNIT	AVAILABLE TECH
		Height of joint 4 of outlet pipe.	m [ft]	LIDAR, Structure from Motion, WSN (displacement)
		Length of segment LO45.	m [ft]	LIDAR, Structure from Motion, WSN (displacement), DSS
		Type of joint at node 4 for outlet pipe.	-	-
		Type of joint at node 5 for outlet pipe.	-	-
	INLET PIPE	Height of joint 1 of inlet pipe (% of Hpv [0-1])	%	LIDAR, Structure from Motion, WSN (displacement)
		Length of segment LO12 (% of Dpv)	%	LIDAR, Structure from Motion, WSN (displacement), DSS
		Type of joint at node 5 for inlet pipe	-	-
	WELLHEAD TREE	Total height of the wellhead aboveground	m [ft]	LIDAR, Structure from Motion, WSN (displacement)
		Height of the horizontal section	m [ft]	LIDAR, Structure from Motion, WSN (displacement)
		Average stiffness of the wellhead	kN/m [kip/inch]	-
		Linear mass of the wellhead tree	kg/m [kip/inch]	-
		Length of segment LP_0-1	m [ft]	LIDAR, Structure from Motion, WSN (displacement), DSS
		Length of segment LP_1-2	m [ft]	LIDAR, Structure from Motion, WSN (displacement), DSS
		Length of segment LP_2-3	m [ft]	LIDAR, Structure from Motion, WSN (displacement), DSS
		Length of segment LP_3-4	m [ft]	LIDAR, Structure from Motion, WSN (displacement), DSS
		Type of joint at node 1	-	-
		Type of joint at node 2	-	-
		Type of joint at node 3	-	-
		Type of joint at node 4	-	-

VARIABLES		DESCRIPTION	UNIT	AVAILABLE TECH
OUTPUT		Strains	%	DSS, WSN (Strain gauge)
		Epistemic uncertainty	-	-

All variables and references used for description in this table correspond to Task D report

Task F – Synthesis of Component Fragilities into a System Performance Model

Buried Pipelines

Figure 36 presents the suggested lognormal cumulative distribution functions (CDFs) for the tensile strain damage state fragility functions assuming a constant aleatory variability, σ = 0.30, for both leakage and rupture, which was estimated using expert opinion (Abrahamson, 2022). The 10th and 90th percentiles are presented for the fragility functions assuming constant epistemic uncertainty, σ_{epi}=0.20, a common assumption for structural systems. σ represents the aleatory variability in the fragility models due to inherent randomness in the loading conditions (e.g., eccentricities in the pipe alignment, nonuniform backfill soil conditions) and pipe properties (e.g., post-yield stress-strain behavior, weld quality, corrosion). To account for greater uncertainty associated with field conditions, the aleatory variability, σ, is increased from 0.407 to 0.50.

Figure 36: Tensile Damage State Fragility Model

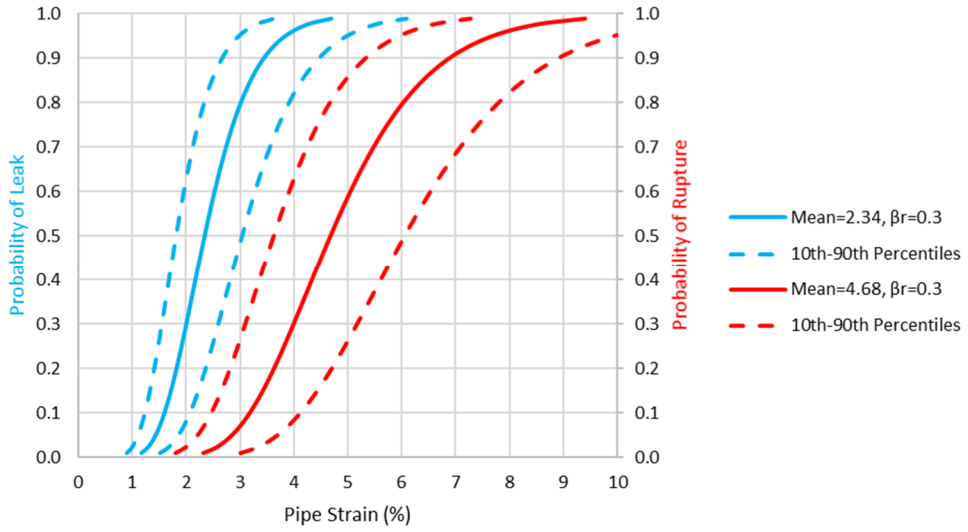

Pipelines can often sustain more axial strain after the initiation of buckling or pipe wall wrinkling before pipe wall tearing or rupturing occurs. The probability of compressive rupture (due to buckling or pipe wall wrinkling) fragility function accounts for this additional capacity by shifting the 50% probability of exceedance values in the original fragility function up to the 20% probability of exceedance level in the final function. Additional details of the pipeline fragility models are provided in Appendix D in Bain et al. (2022). Figure 37 depicts the fragility model for compressive ruptures.

Figure 37: Probability of Compressive Rupture for Select D/t Ratios

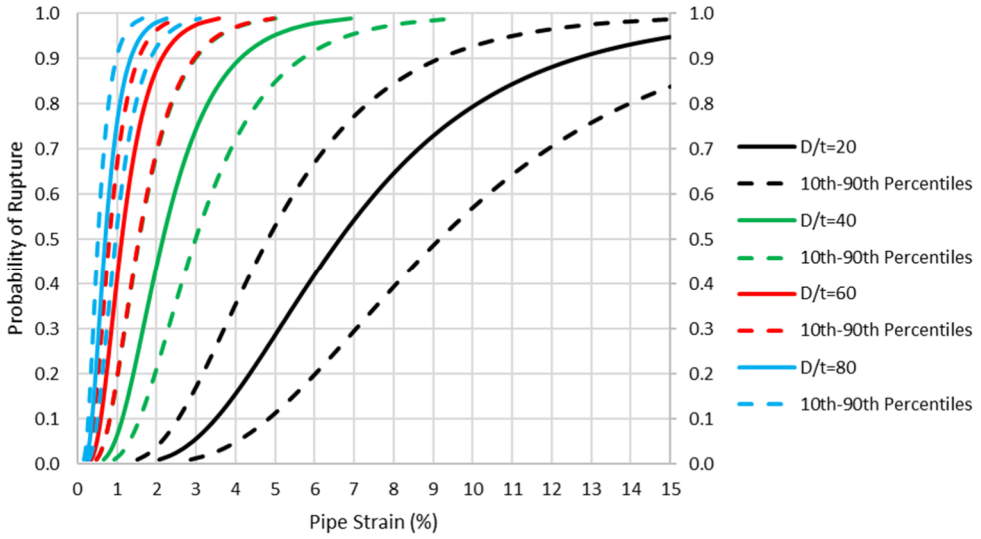

Fault Shear Induced Failure on Wells

The probability of failure given fault-displacement induced shear strain is presented in Figure 38.

Figure 38: Probability of Failure for Well Casing and Tubing due to Fault Offset

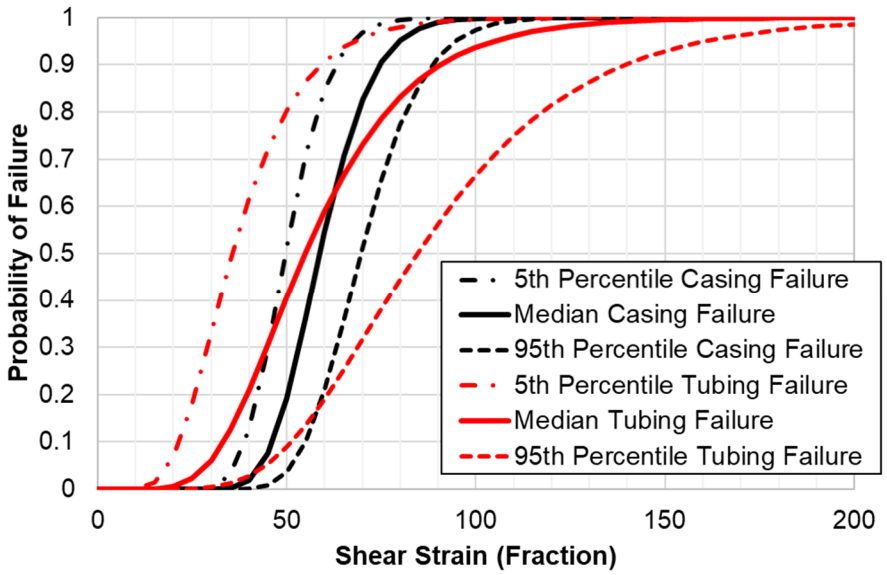

Shaking Induced Failure on Wells

The probability of ground shaking induced failure is plotted in Figure 39 through Figure 42 for the conductor casing, production casing, surface casing, and well tubings. The median plastic moment at which 50% probability of failure occurs is compiled and estimated by the Task C researchers.

Figure 39: Probability of Failure for Conductor Casing due to Ground Shaking

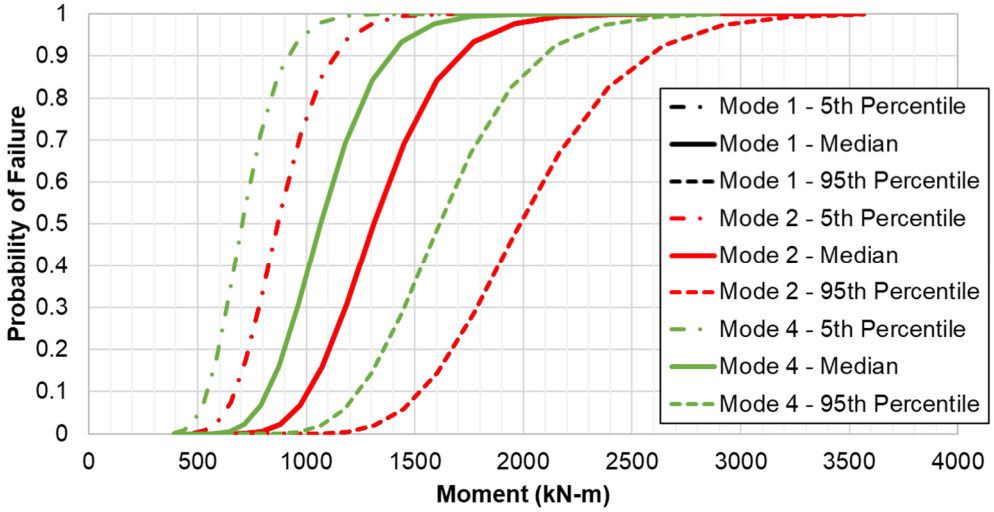

Figure 40: Probability of Failure for Surface Casing due to Ground Shaking

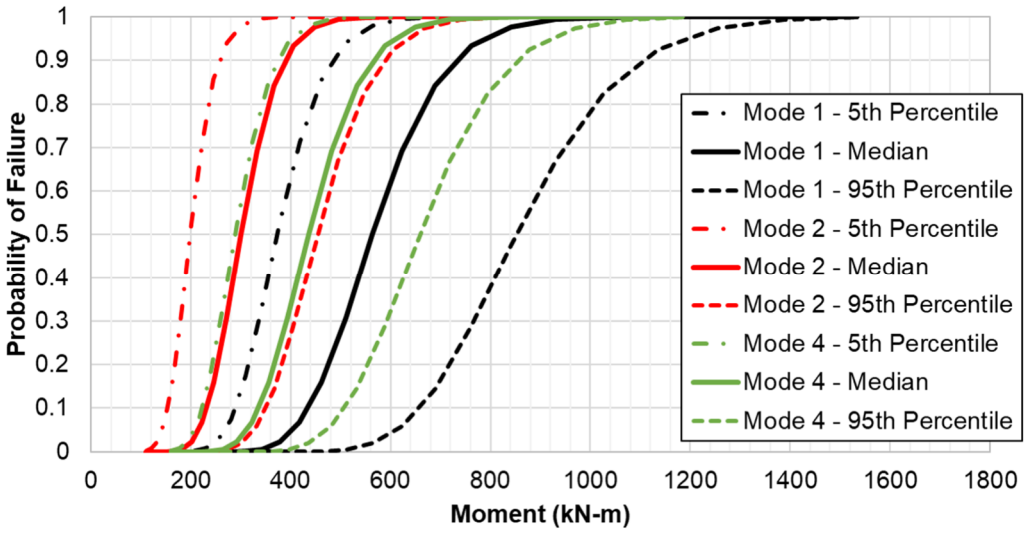

Figure 41: Probability of Failure for Production Casing due to Ground Shaking

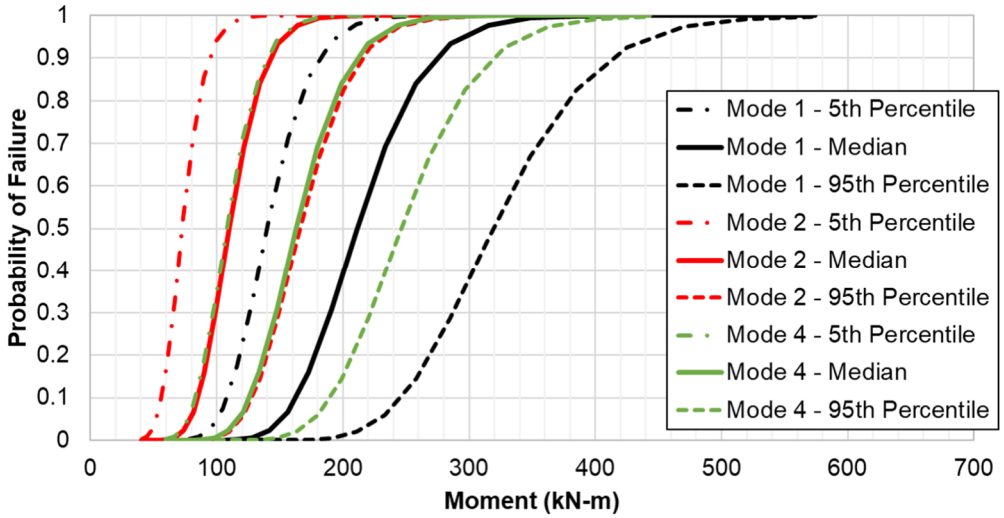

Figure 42: Probability of Failure for Tubing due to Ground Shaking

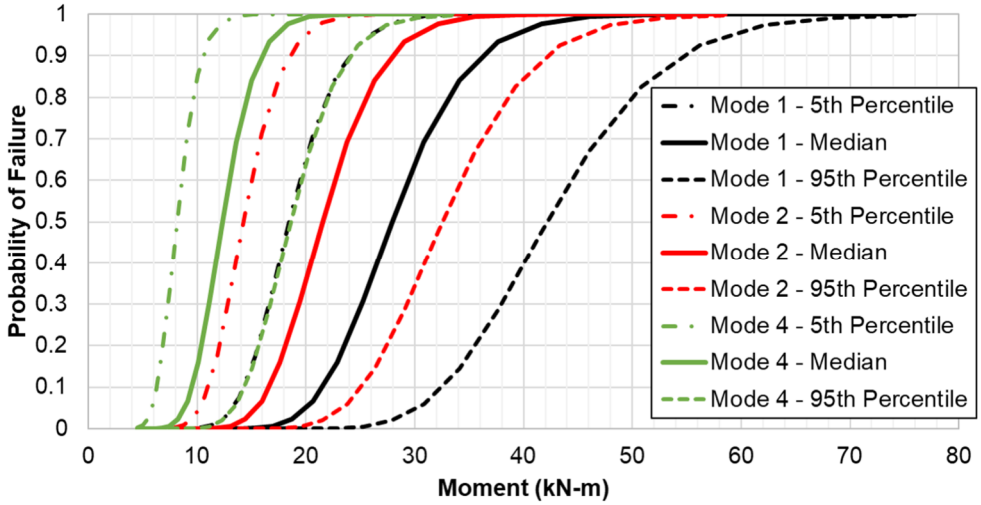

Fault Shear Induced Failure on Caprocks

Based on the finite element modeling performed under Task C, caprocks proved to be insensitive to most of the input parameters. As such, the only parameter taken into account is if a fault crosses the caprock. If caprock-fault crossing exists, then the average probability of leakage for caprocks is 8.9%, with σ_{epi} of 0.86%.

Aboveground Systems

The models for failure of aboveground components are dependent on ground shaking. As seismic hazards are distributed over an area, all aboveground components that are within 200 km of each fault trace will be evaluated for ground shaking induced failure.

Well tree

As described previously and in Watson-Lamprey et al. (2022), methodologies for probability of failure provided for well trees fall into six cases, these cases are further split up based on direction of ground motion. In total there are 22 unique models that may need to be computed to the distribution of joint rotation over the six subsystem-component combination (examples of

these rotation models are shown in Figure 34). Each of the rotation models are then propagated into models for longitudinal strain, and subsequently the probability of failure given longitudinal strain. Once the probability of failure for a specific subsystem-component combination, direction of shaking, joint location, and orientation is determined, then the distributions of probability of failure for all variations within each subsystem-component combination are averaged to obtain the overall average distribution for probability of failure. Figure 43 shows the probability of failure for wellheads due to ground shaking (along with the 5th and 95th percentiles).

Figure 43: Probability of Failure for Wellheads due to Ground Shaking

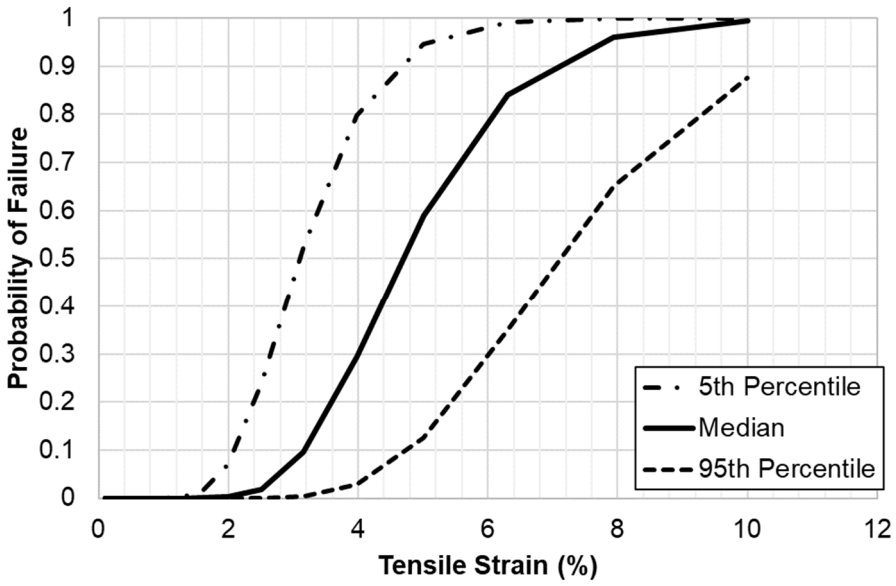

Pressure Vessels

For the pressure vessels, the critical component considered was the base of the pressure vessel. Two types of base connections were considered. The first represents the configuration of older pressure vessels, in which the base anchors are embedded in a concrete footing and thus designed as a fully fixed connection. In this case, no elongation of the anchor will occur, and minimal base rotation is anticipated, consequently the base of these pressure vessels is considered fixed. This case is labeled as “no stretch length”. The second configuration is typical of newer pressure vessels. In this case, the anchors have a designed free stretch length of at least eight times the diameter of the anchor. This allows the base to rotate, hence a nonlinear spring is incorporated in the model at the base of the vessel. The distribution of the probability of failure for pressure vessels with ground shaking is shown in Figure 44.

Figure 44: Probability of Failure for Pressure Vessels due to Ground Shaking

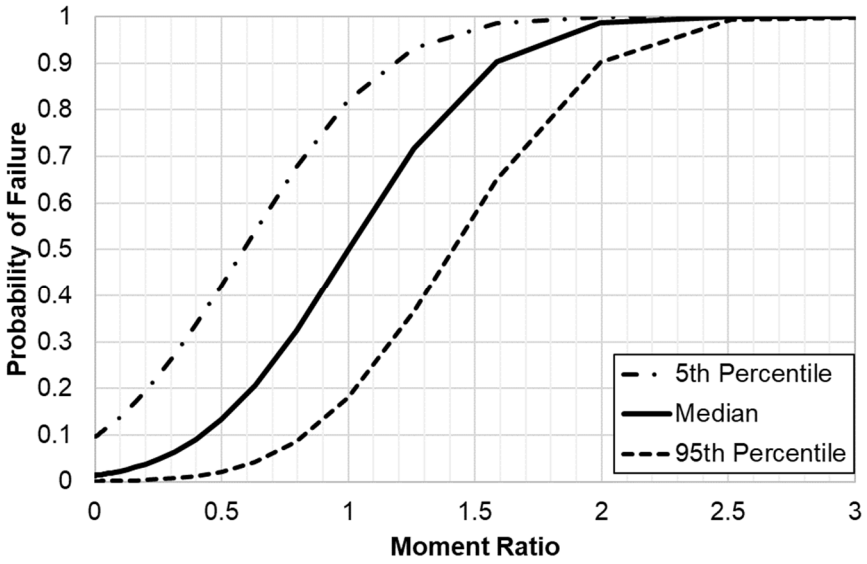

OpenSRA Graphical User Interface

The final component of *OpenSRA*, and the aspect that brings the backend calculations together is the graphical user interface (GUI). Further information about the graphical user interface and instructions on its use can be found in the User Manual.

The user interface consists of multiple tabs that follow the PBEE framework. The visualization tab shows the inputs (infrastructure, ground motion, faults, and base maps) and will update once the analysis is performed. Figure 45 depicts a representative view of the GUI, showing PGA contours of the South Napa (2014) ShakeMap and the publicly available transmission line database.

Figure 45: Screenshot of Graphical User Interface

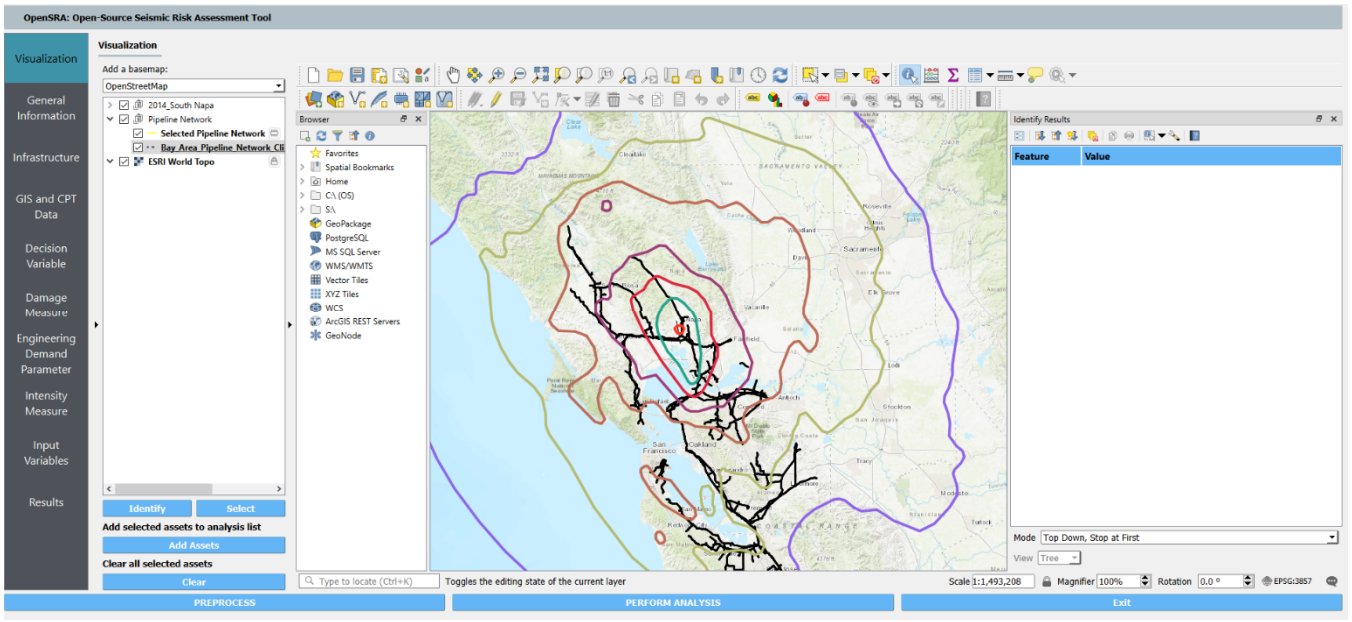

Example using the California Public Transmission Line Network with a USGS ShakeMap to predict the probability of failure of buried pipelines. The black lines depict the pipeline network and the colored contours are PGA of the ShakeMap.

Project Metrics

Metric goals were established at the beginning of the project to monitor the successful progress of the project: website clicks, User Workshop attendance, lab testing goals, and validation results. These metrics are associated with project exposure, interest and utilization of the software, and improvement of calculation methods.

This project met and exceeded these metrics. The interest in *OpenSRA* has grown; the number of project website clicks at the end of 2022 exceeds the goal by a factor of 33. The User Workshop had around 80 registrations globally, with 31 in-person attendees; the in-person attendees benefitted from the hands-on software demonstrations. The number of lab test configurations exceeded the target goal by 30%. More information about knowledge transfer can be found in Kang et al. (2023). Validation of the software was conducted at four demonstration sites, and the *OpenSRA* results correlated well with documented observations after selected earthquakes or test earthquake events. More information about validation can be found in Bain et al. (2023).

Conclusion

The project developed new seismic risk assessment methods (both demand and fragility functions of components) and implemented these into an open-source seismic risk assessment software called *OpenSRA*. The project was split into six task groups to assess the seismic demands imposed on gas infrastructure and the seismic fragility of individual components. The project teams provided guidance on how to calculate the probability of failure for different components of the gas system. This guidance was based on thorough literature reviews, discussions with utility owners, data analysis, laboratory testing, and finite element modeling.

The primary result of this project is the user-friendly open-source seismic risk software for gas pipelines and storage facilities called *OpenSRA*. It is available to the public through the PEER website. The *OpenSRA* software addresses several of the concerns associated with the ad hoc way current seismic risk assessments of gas pipelines and storage facilities are performed.

The Performance-Based Earthquake Engineering (PBEE) framework is implemented in the OpenSRA software through fragility curves that describe the seismic performance of key gas infrastructure components. The fragility curves were developed through state-of-the-art numerical modeling efforts based on how system components respond to earthquake hazards. The developed models incorporate comprehensive inventories of fault and pipeline crossings for California using the Quaternary Faults and Fold database and incorporate geologic, subsurface, and topographic data required in updated earthquake hazard regional scale assessments.

The end products given for seismic demands included a fault-pipeline crossing database, methods to estimate primary and secondary fault displacement hazard, and methods to estimate geohazard-induced by seismicity. Fragility curves were developed for buried pipelines, wells and caprocks, and aboveground gas infrastructure. These seismic demand and fragility elements were then utilized within the PBEE framework to estimate the probability of failure given an earthquake scenario. The developed *OpenSRA* software provides a user interface to allow utility owners to utilize all these calculations and findings to help prioritize mitigation efforts on their gas infrastructure.

To perform the calculations within *OpenSRA* in a timeframe that will be useful to the user, a novel method called Polynomial Chaos (PC) was implemented. This methodology can employ clearly defined means, aleatory variabilities, and epistemic uncertainties for each step of the Performance-Based Earthquake Engineering risk methodology to deliver results rapidly. The use of PC over traditional Monte-Carlo sampling can easily improve the computation time by two to three orders of magnitude.

Improved models of earthquake-induced ground failure hazards (i.e., liquefaction-induced lateral spreading and earthquake shaking-induced landslides) were developed to better capture these hazards at different levels of regional scale analysis. The uncertainty assigned to the ground failure hazard models at different regional scales are consistent with the information available in California at the state-wide, regional, and site-specific levels.

Experiments of pipe component system provided critical insights on their seismic performance. Advanced analysis of gas storage wells identified key response characteristics and insights on their seismic performance.

New sensing technologies were identified which can inform the risk models at the input, intermediate, and final output stages. The selected sensing technologies can be categorized into four main categories: 1. Remote sensing technologies, 2. Continuous monitoring technologies, 3. Inspection technologies, and 4. Leakage detection technologies. They were selected depending on the employed *OpenSRA* parameters, which include available geologic information and characteristics of the gas infrastructure.

The *OpenSRA* software helps utility owners assess their infrastructure both pre- and post-earthquake. It also provides a consistent means for regulators to assess the seismic risk of the gas infrastructure in California. The software helps prioritize mitigation efforts of potentially vulnerable systems before an earthquake utilizing ground motion prediction equations and past earthquake ShakeMaps. After a seismic event occurs *OpenSRA* also allows the end-user to assess potential leaks and breaks in the system to send out relief efforts quickly. This ability to not only prioritize mitigation efforts prior to an earthquake, but also help prioritize larger potential breaks after an event allows utility owners to protect their constituents from potentially catastrophic failures. Along with this, these mitigation efforts reduce environmental impacts and allow for efficient planning and construction to occur on new gas infrastructure.

Given the focused timeframe of the project, and the lack of existing fragility curves currently available, this project focused on common infrastructure to be broadly applicable. *OpenSRA* would benefit from additional research to:

1. Integrate directly with the USGS for ShakeMap scenarios.
2. Develop and incorporate additional ground failure hazard demand models.
3. Extend numerical models of soil-pipeline response to capture additional pipe systems and soil conditions for additional loading scenarios such as distributed shear.
4. Develop fragility functions for components not investigated in this research project, such as the performance of pipelines attached to bridges crossing rivers.
5. Additional pipe component and system testing to refine their fragility functions.
6. Allow for more flexibility in input datasets.
7. Develop more flexible output system for users to choose what to receive.
8. Integrate network/flow analysis into infrastructure types that have upstream/downstream dependencies.
9. Allow for more complex rupture scenarios (in addition to simple fault plane geometries).
10. Integrate other forms of natural hazards in addition to the seismic hazard.
11. Further develop the backend to make better use of computer resource for computational efficiency.
12. Develop cloud-/server-based dissemination of datasets and updates or extend the application to be web-based for broader access.
13. Install sensing technologies in a variety of gas infrastructure systems to evaluate their performance over an extended period.
14. Develop methodologies to optimize the updating of models using information from sensors on gas infrastructure.

It is the hope of the research team to continue to expand the use of *OpenSRA* through additional research projects in the future.

Acknowledgements

The authors want to recognize the California Energy Commission and thank the Commission for recognizing how vital this research is to the industry. We would like to thank them for funding this project and giving us the opportunity to refine current practice with more in-depth research. Specifically, we would like to thank Dr. Yahui Yang, the project manager from the California Energy Commission, for providing guidance throughout the process of developing the interim reports and final report.

Prof. Jonathan Bray of University of California, Berkeley is the PI of the project and Dr. Jennie Watson-Lamprey of Slate Geotechnical Consultants is the Project Manager. Dr. Watson-Lamprey with Micaela Largent and Dr. Barry Zheng of Slate Geotechnical Consultants helped us organize our collaborations with the different research teams. These included Task A (Prof. Norm Abrahamson, Dr. Maxime Lacour, and Dr. Steve Thompson), Task B (Prof. Jonathan Bray, Chris Bain, Dr. Daniel Hutabarat, Prof. Thomas O'Rourke, and Scott Lindvall), Task C members (Dr. Jonny Rutqvist, Dr. Keurfon Luu, Preston Jordan, Dr. Tsubasa Sasaki, Dr. William Foxall and Dr. Yingqi Zhang), Task D members (Prof. Tara Hutchinson, Prof. David McCallen, Prof. Sherif Elfass, Dr. Elide Pantoli and Dr. Suiwen Wu), and Task E members (Dr. Kenichi Soga, Dr. James Wang, Peter Hubbard, and Tiachen Xu). Dr. Stevan Gavrilovic, Dr. Sanjay Govindjee, Dr. Frank McKenna, Dr. Matthew Schoettler of the NHERI SimCenter at UC Berkeley provided software development support. Grace Kang, Dr. Amarnath Kasalanati, and Dr. Arpit Nema of the Pacific Earthquake Engineering Research Center (PEER) provided outreach, administrative, and technical support of the project. Shakhzod Takhirov, Llyr Griffiths, and Matt Cataleta of UC Berkeley's Civil Engineering laboratories also supported the demonstration testing.

Pacific Gas and Electric Company and the East Bay Municipal Utility District donated testing samples. Dr. Sjoerd van Ballegooy and his staff at Tonkin & Taylor, Ltd. of New Zealand shared data and insights on the ground characterization and ground performance data of the Canterbury Earthquake Sequence. Tim McCrink and Dr. Erik Frost from the California Geological Survey provided a database of rock strength test results and insights into regional slope stability and displacement analyses in California. Dr. Christina Argyrou and Dr. Dilan Roberts shared their experience with Abaqus and its models. Prof. Katerina Ziotopoulou and Renmin Pretell of University of California, Davis provided invaluable insights into the soil performance at the Balboa Boulevard demonstration site during the Northridge earthquake. Dr. Craig Davis provided strength test data for the Granada water trunk line at Balboa Boulevard and insights into evaluating uncertainty in pipeline material properties. Amy Frithsen managed the grant and contracts through ERSO at UC Berkeley.

The authors thank the project partners of Pacific Gas and Electric Company (PG&E) and Southern California Gas Company (SoCalGas) for sharing data, insights, and technical advice throughout the project, with particular thanks to Dr. Chris Madugo, Dr. Albert Kottke, Dr. Masoud Poul, Nozar Jahangir, Jeremy Dong, Dr. Masoud Mogtarderi-Zadeh, Jeffrey Bachhuber, and the technical staff at PG&E.

This research study was funded by the California Energy Commission, under Contract No. PIR 18-003. The opinions, findings, conclusions, and recommendations expressed in this publication are those of the authors and do not necessarily reflect the view of California Energy Commission and its employees, the State of California, the Pacific Earthquake Engineering Research (PEER) Center, and the Regents of the University of California.

References

Abrahamson, N.A., Silva, W.J., Kamai, R. (2014). Summary of the ASK14 Ground Motion Relation for Active Crustal Regions: Earthquake Spectra, v. 30, no. 3, p. 1025-1155.

Abrahamson, N. (2022). Personal Communication.

Bain, C., D. Hutabarat, J.D., Bray, N., Abrahamson, T.D., O'Rourke, S., Lindvall (2022). Performance-Based Earthquake Engineering Assessment Tool for Natural Gas Storage and Pipeline Systems, Task B - Enhanced Liquefaction and Ground Deformation Report. California Energy Commission.

Bain, C., T.D., O'Rourke, J., Bray, B., Zheng, D., Hutabarat, S., Lindvall, P., Jordan, T., Sasaki, K., Luu, Y., Zhang, W., Foxall, J., Rutqvist, D., McCallen, S., Elfass, T., Hutchinson, E., Pantoli (2023). Performance-Based Earthquake Engineering Assessment Tool for Natural Gas Storage and Pipeline Systems, Validation Report. California Energy Commission.

Boore, D.M., Stewart J.P., Seyhan, E., and Atkinson, G.M., 2014, NGA-West2 Equations for Prediction PGA, PGV, and 5%-Damped PSA for Shallow Crustal Earthquakes: Earthquake Spectra, v. 30, no. 3, p. 1057-1085.

Boulanger, R. W., and I.M., Idriss (2016). CPT-based liquefaction triggering procedure. Journal of Geotechnical and Geoenvironmental Engineering, 142(2), 04015065-04015065.

Bray, J. D., and J., Macedo (2019). Procedure for estimating shear-induced seismic slope displacement for shallow crustal earthquakes. Journal of Geotechnical and Geoenvironmental engineering, 145(12), 04019106.

Campbell, K.W., and Bozorgnia, Y. (2014). NGA-West2 Ground Motion Model for the Average Horizontal Component of PGA, PGV and 5% Damped Linear Acceleration Response Spectra: Earthquake Spectra, v. 30, no. 3, p. 1087-1115.

Cetin, K. O., H.T., Bilge, J., Wu, A.M., Kammerer, and R.B., Seed (2009). Probabilistic model for the assessment of cyclically induced reconsolidation (volumetric) settlements. Journal of Geotechnical and Geoenvironmental Engineering, 135(3), 387.

Chiou, B.S., and Youngs, R.R. (2014). Update of the Chiou and Youngs NGA Model for the Average Horizontal Component of Peak Ground Motion and Response Spectra: Earthquake Spectra, v. 30, no. 3, p. 1117-1153.

Cornell, C.A. (1968). Engineering seismic risk analysis: Bulletin of the Seismological Society of America, v. 58, p. 1583–1606.

Elfass S., E., Pantoli, D., McCallen, T.C., Hutchinson (2023). Shake Table Testing of a Surface Natural Gas Piping Subsystem. A Report for the "Performance-based Earthquake Engineering Assessment Tool for Natural Gas Storage and Pipeline Systems" Project. PEER Report No. 2023/X. Pacific Earthquake Engineering Research Center, University of California, Berkeley, CA. https://doi.org/X.

Field, E.H., Biasi, G.P., Bird, P., Dawson, T.E., Felzer, K.R., Jackson, D.D, Johnson, K.M., Jordan, T.H., Madden, C., Michael, A.J., Milner, K.R., Page, M.T., Parson, T., Powers, P.M., Shaw, B.E., Thatcher, W.R., Weldon, J.J. II, and Zeng, Y. (2013). Uniform California Earthquake Rupture Forecast, Version 3 (UCERF3) – The Time-Independent Model: U.S. Geological Survey Open-File Report 2013-1165.

FEMA (2020). Hazus 4.2 SP3 Technical Manual. Federal Emergency Management Agency. https://www.fema.gov/sites/default/files/2020-10/fema_hazus_earthquake_technical_manual_4-2.pdf

Grant, A., J., Wartman, and G., Abou-Jaoude (2016). Multimodal method for coseismic landslide hazard assessment. Engineering Geology, 212, 146-160.

Holzer, T. L., T.E., Noce, and M.J., Bennett (2011). Liquefaction Probability Curves for Surficial Geologic Deposits. Environmental and Engineering Geoscience, 17(1), 1–21. doi: 10.2113/gseegeosci.17.1.1

Hutabarat, D., T.D., O'Rourke, J.D., Bray, C., Bain, S., Lindvall (2023). Performance-Based Earthquake Engineering Assessment Tool for Natural Gas Storage and Pipeline Systems, Underground Pipeline Fragilities. PEER Report No. 2023/X. Pacific Earthquake Engineering Research Center, University of California, Berkeley, CA. https://doi.org/X.

Idriss, I.M., & R.W., Boulanger (2008). Soil Liquefaction During Earthquakes. EERI Publication, Monograph MNO-12, Earthquake Engineering Research Institute, Oakland.

Idriss, I.M, and J.I., Sun (1993). User's manual for SHAKE91: A computer program for conducting equivalent linear seismic response analyses of horizontally layered soil deposits. Center for Geotechnical Modeling, University of California, Davis.

Itasca Consulting Group (2020). FLAC3D — Fast Lagrangian Analysis of Continua in Three-Dimensions, Ver. 7.0. https://www.itascacg.com/software/FLAC3D.

Kang, G., J., Watson-Lamprey, M., Largent (2023). Performance-Based Earthquake Engineering Assessment Tool for Natural Gas Storage and Pipeline Systems, Knowledge Transfer Final Report. California Energy Commission.

Ku, C. S., C.H., Juang, C.W., Chang, and J., Ching (2012). Probabilistic version of the Robertson and Wride method for liquefaction evaluation: development and application. Canadian Geotechnical Journal, 49(1), 27-44.

Lacour, M., and N., Abrahamson (2021). Efficient Propagation of Epistemic Uncertainty for Probabilistic Seismic Hazard Analyses (PSHAs) Including Partial Correlation of Magnitude–Distance Scaling. Bulletin of the Seismological Society of America, 111(6), 3332-3340.

Lacour, M., and N., Abrahamson (2023). Efficient Risk Calculation for Performance-Based Earthquake Engineering Distributed Systems. A Report for the "Performance-based Earthquake Engineering Assessment Tool for Natural Gas Storage and Pipeline Systems" Project. PEER Report No. 2023/X. Pacific Earthquake Engineering Research Center, University of California, Berkeley, CA. https://doi.org/X.

Luu, K., P., Jordan, W., Foxall, J., Rutqvist (2023). Dynamic seismic analysis of wellbore integrity. A Report for the "Performance-based Earthquake Engineering Assessment Tool for Natural Gas Storage and Pipeline Systems" Project. PEER Report No. 2023/X. Pacific Earthquake Engineering Research Center, University of California, Berkeley, CA. https://doi.org/X.

McKenna, F. (2011). OpenSees: A framework for earthquake engineering simulation. Computing in Science & Engineering 13(4):58–66. doi: 10.1109/MCSE.2011.66.

Moehle, J., & G.G., Deierlein (2004). A framework methodology for performance-based earthquake engineering. 13th World Conference on Earthquake Engineering Proceedings (Vol. 679). Vancouver: WCEE, August 2004.

Moss, R. E., R.B., Seed, R.E., Kayen, J.P., Stewart, A., Der Kiureghian, and K.O., Cetin (2006). CPT-based probabilistic and deterministic assessment of in situ seismic soil liquefaction potential. Journal of Geotechnical and Geoenvironmental Engineering, 132(8), 1032-1051.

Pantoli, E., T.C., Hutchinson, S.A., Elfass, and D.B., McCallen (2022). Performance-Based Earthquake Engineering Assessment Tool for Natural Gas Storage and Pipeline Systems, Task D Final Report - Seismic Response of Pipeline and Gas Storage Surface Infrastructure. California Energy Commission.

Petersen, M. D., T. E. Dawson, R. Chen, T. Cao, C. J. Wills, D. P. Schwartz, and A. D. Frankel. (2011). Fault displacement hazard for strike-slip faults: Bulletin of the Seismological Society of America, v. 101, pp. 805–825.

Pruess, K., C. Oldenburg, and G. Moridis (2011). TOUGH2 User's Guide, Version 2. LBNL-43134. Lawrence Berkeley National Laboratory, CA.

Robertson, P. K. (2009). Interpretation of cone penetration tests—a unified approach. Canadian geotechnical journal, 46(11), 1337-1355.

Robertson, P. K., & C.E., Wride (1998). Evaluating cyclic liquefaction potential using the cone penetration test. Canadian geotechnical journal, 35(3), 442-459.

Rockpoint Gas Storage. Lodi. Retrieved March 2021, from https://www.rockpointgs.com/Businesses/Lodi

Rutqvist, J., T., Sasaki, L., Luu, P., Jordan, Y., Zhang, W., Foxall, J., Watson-Lamprey, M., Largent, B., Zheng, (2022). Performance-Based Earthquake Engineering Assessment Tool for Natural Gas Storage and Pipeline Systems, Task C Final Report - Seismic Response of Wells and Caprocks. California Energy Commission.

Sasaki, T., P., Jordan, W., Foxall, and J., Rutqvist (2023). Fragility of Wells due to Fault Shearing—The Impact of Fault Displacement on the Integrity of Natural Gas Storage Wells in California. A Report for the "Performance-based Earthquake Engineering Assessment Tool for Natural Gas Storage and Pipeline Systems" Project. PEER Report No. 2023/X. Pacific Earthquake Engineering Research Center, University of California, Berkeley, CA. https://doi.org/X.

Smith M. (2009). Abaqus/Standard User's Manual, Version 6.9.

SoCalGas (2016). How Underground Natural Gas Storage Works. Retrieved March 17, 2022, from https://www.youtube.com/watch?v=3FSMpCazwUA.

Thompson, Stephen. (2021). Fault Displacement Hazard Characterization for OpenSRA. California Energy Commission.

U.S. Geological Survey and California Geological Survey (USGS and CGS). (2006). Quaternary Fault and Fold Database of the United States: url http://earthquake.usgs.gov/hazards/qfaults/; accessed 3/13/2019.

Wald, D. J., B.C., Worden, V., Quitoriano, amd K.L., Pankow (2005). ShakeMap manual: technical manual, user's guide, and software guide (No. 12-A1).

Wang, C., P., Hubbard, T., Xu, K., Soga (2021). Performance-Based Earthquake Engineering Assessment Tool for Natural Gas Storage and Pipeline Systems, Task 4E Final Report – Sensor and Monitoring Technologies. California Energy Commission.

Watson-Lamprey, J., M., Largent, B., Zheng (2022). System Wide Natural Gas Infrastructure Response and Fragility Model. California Energy Commission.

Wells, D. L., and K. J. Coppersmith. (1994). New empirical relationships among magnitude, rupture length, rupture width, rupture area, and surface displacement: Bulletin of the Seismological Society of America, v. 84, pp. 974–1002.

Youd, T. L., and D.M., Perkins (1978). Mapping liquefaction-induced ground failure potential. Journal of the Geotechnical Engineering Division, 104(4), 433-446.

Zhang, G., P.K., Robertson, and R.W.I., Brachman (2002). Estimating Liquefaction-Induced Ground Settlements from CPT for Level Ground. Canadian Geotechnical Journal, 39(5), 1168–1180. doi: 10.1139/t02-047

Zhang, Y., K., Ma, S., Song, M.B., Elam, G.A., Cook, & E.A., Park (2004). Peroxisomal proliferator-activated receptor-γ coactivator-1α (PGC-1α) enhances the thyroid hormone induction of carnitine palmitoyltransferase I (CPT-Iα). Journal of Biological Chemistry, 279(52), 53963-53971.

Zhang, Y., P., Jordan, W., Foxall, J., Rutqvist (2023). Fragility Analysis Related to Caprock Leakage from Underground Gas Storage Reservoirs. A Report for the “Performance-based Earthquake Engineering Assessment Tool for Natural Gas Storage and Pipeline Systems” Project. PEER Report No. 2023/X. Pacific Earthquake Engineering Research Center, University of California, Berkeley, CA. https://doi.org/X.

Zheng, B., M., Largent, T., Clifford, J., Watson-Lamprey (2023). Draft OpenSRA Report. California Energy Commission.

Zhu, J., L.G., Baise and E.M., Thompson (2017). An Updated Geospatial Liquefaction Model for Global Application. Bulletin of the Seismological Society of America, 107(3), 1365–1385. doi: 10.1785/0120160198

Zhu, M., F., McKenna, & M.H., Scott (2018). “OpenSeesPy: Python Library for the OpenSees Finite Element Framework.” SoftwareX 7:6–11. doi: 10.1016/j.softx.2017.10.009.

Project Deliverables

The following project deliverables, including additional interim reports not listed below, are available upon request by submitting an email to pubs@energy.ca.gov. These deliverables can also be found at the project website https://www.peer.berkeley.edu/OpenSRA.

- Final Report
- *OpenSRA* Report
- *OpenSRA* Manual
- Fault Displacement Hazard Model Report
- Enhanced Regional Liquefaction and Ground Deformation Report
- Seismic Response of Wells and Caprocks Report
- Seismic Response of Pipeline and Gas Storage Surface Infrastructure Report
- Sensor and Monitoring Technologies Report
- Report of System Wide Natural Gas Infrastructure Response and Fragility Model
- Conceptual Design, Use Cases. and Development Plan Memorandum
- Validation Report
- Seismic risk analysis tool *OpenSRA*

-